Contents lists available at ScienceDirect

EBioMedicine

journal homepage: www.elsevier.com/locate/ebiom

Research paper

Epigenetic activation of O-linked β-N-acetylglucosamine transferase overrides the differentiation blockage in acute leukemia

K.M. Kampa-Schittenhelm[a,*], T. Haverkamp[b], M. Bonin[c], V. Tsintari[a], H.J. Bühring[a],
L. Haeusser[a], G. Blumenstock[d], S.T. Dreher[a], T. Ganief[e], F. Akmut[a], B. Illing[a],
U.A. Mau-Holzmann[h], I. Bonzheim[f], E. Schleicher[g], W. Vogel[a], M.M. Schittenhelm[a,i]

[a] University Hospital Tübingen, Dept. of Hematology, Oncology, clinical Immunology and Rheumatology, Otfried-Müller-Straße 10, BB West, Rooms 585-587, 72076 Tübingen, Germany
[b] Labor Eberhard & Partner, Dortmund, Germany
[c] Microarray Genechip Facility Tübingen and Institute for Medical Genetics and Applied Genomics, Germany
[d] Institute of Clinical Epidemiology and Applied Biometry, Eberhard Karls University Tübingen, Germany
[e] Proteome Center Tübingen at the University of Tübingen, Germany
[f] Institute of Pathology at the University Hospital Tübingen, Germany
[g] University Hospital Tübingen, Dept. of Diabetology, Endokrinology, Nephrology, Germany
[h] University Hospital Tübingen, Division of Cytogenetics, Institute for Medical Genetics and Applied Genomics, Germany
[i] Clinic of Medical Oncology and Hematology, Cantonal Hospital St. Gallen (KSSG), Switzerland

ARTICLE INFO

ABSTRACT

Background: Overriding the differentiation blockage in acute myeloid leukemia (AML) is the most successful mode-of-action in leukemia therapy – now curing the vast majority of patients with acute promyelocytic leukemia (APL) using all-trans retinoic acid (ATRA)-based regimens. Similar approaches in other leukemia subtypes, such as IDH1/2-mutated AML, are under active investigation. We herein present successful release of the differentiation blockage upon treatment with the natural $(-)$-Δ^9-Tetrahydrocannabinol isomer dronabinol *in vitro* and *in vivo*.

Methods: Cellular maturation and differentiation were followed in two patients employing whole genome methylation profiling, proteome analyses, NGS deep sequencing and multispectral imaging flow cytometry. For functional studies lentiviral OGT knock-down *in vitro* and *ex vivo* cell models were created to evaluate proliferative, apoptotic and differentiating effects of OGT in acute leukemia.

Findings: In here, we provide molecular evidence that dronbinol is capable to override the differentiation blockage of acute leukemia blasts at the state of the leukemia-initiating clone. We further identify the O-linked β-N-acetyl glucosamine (O-GlcNAc) transferase (OGT) to be crucial in this process. OGT is a master regulator enzyme adding O-GlcNAc to serine or threonine residues in a multitude of target proteins. Aberrant O-GlcNAc modification is implicated in pathologies of metabolic, neurodegenerative and autoimme diseases as well as cancers. We provide evidence that dronabinol induces transcription of *OGT* via epigenetic hypomethylation of the transcription start site (TSS). A lentiviral OGT-knock out approach proves the central role of OGT exerting antileukemic efficacy via a dual-mechanism of action: High concentrations of dronabinol result in induction of apoptosis, whereas lower concentrations drive cellular maturation. Most intriguingly, overriding of the differentiation blockage of acute leukemia blasts is validated *in vivo* following two patients treated with dronabinol.

Interpretation: In conclusion, we provide evidence for overcoming the differentiation blockage in acute leukemia in subentities beyond promyelocytic and IDH1/2-mutated leukemia and thereby identify O-GlcNAcylation as a novel (drugable) field for future leukemia research.

Funding: Unrestricted grant support by the IZKF Program of the Medical Faculty Tübingen (MMS) and Brigitte Schlieben-Lange Program as well as the Margarete von Wrangell Program of the Ministry of Science, Research and the Arts, Baden-Württemberg, Germany (KKS) and Athene Program of the excellence initiative University of Tübingen (KKS).

* Corresponding author.
  E-mail address: kerstin.kampa-schittenhelm@med.uni-tuebingen.de
(K.M. Kampa-Schittenhelm).

Research in context

Before the study, effects of cannabinoids on cellular differentiation of leukemic blasts were not known.

Added value of this study

This study confirms clinical efficacy of dronabinol in acute leukemia, following the course of disease of two patients with T-ALL, resp. secondary AML. Importantly, a molecular rationale is provided, following a bed-to-bench concept identifying (A) a novel mode-of-action of dronabinol as an unselective epigenetic modifier and (B) O-GlcNAcylation (in competition to phosphorylation) as an important mechanism in leukemogenesis, that may well serve as a potential therapeutic target in acute leukemia. Finally (C), we demonstrate that dronabinol overcomes the differentiation blockage in acute leukemia, which may serve as a novel therapeutic strategy in leukemia subentities similar to promyelocytic and IDH1/2-mutated leukemia as outlined.

Implication of all the available evidence

This study provides a significant impact on the understanding of leukemogenesis and provides a proof-of-concept rationale for further clinical evaluation of cannabinoids in leukemia therapy.

1. Introduction

The current understanding of leukemogenesis is based on an evolutionary process, where stepwise acquisition of somatic mutations drives hematopoietic progenitor/stem cells to malignant transformation, impairing hematopoietic differentiation and control of cellular proliferation and viability [1−3]. Most therapies in oncology aim to (more or less selectively) kill the malignant cells − however, the most successful mode-of-action has been demonstrated in APL via overriding the differentiation blockage of the initiating leukemic clone leading to cure of this highly aggressive malignancy [4]. Release of the differentiation blockage is not unique for APL − but has been observed in other leukemia subentities as well, following treatment with e.g. IDH1/2- or tyrosine kinase inhibitors [5−8] − but efficacies and durable remissions are rather limited as a monotherapy approach.

High hopes are set in these novel inhibitors − and the first FLT3 and IDH1/2 inhibitors have been approved by federal authorities (e.g. FDA, EMA) for the treatment of AML. However, the possibility to induce differentiation of leukemic blasts bears substantial risks (especially differentiation syndrome) and caution and experience are needed when treating patients with such an approach.

A second problem arising from the use of differentiating inhibitors is the long latency of some agents of up to 2 months to clinically verify substantial differentiation − and compounds with potential differentiating capacities may not have been recognized in the past.

We now provide evidence that the natural $(-)$-Δ^9-Tetrahydrocannabinol (THC) isomer dronabinol possesses *in vivo* antileukemic activity − and describe a novel mode of action via epigenetic regulation of OGT-mediated release of the differentiation blockage:

OGT is a master regulator enzyme adding O-GlcNAc to serine or threonine residues in a multitude of target proteins [9,10]. Aberrant O-GlcNAc modification is implicated in pathologies of metabolic and neurodegenerative diseases as well as cancers and autoimmunity. Interestingly, several proteins involved in hematologic malignancies have been reported to directly interact with OGT, such as MLL [11−13], AKT [14], TET2 [15] or ASXL1 [13,16].

We now demonstrate, that dronabinol exerts epigenetic activity with hypomethylation of the 5'UTR/promoter region of *OGT* resulting in an increase of OGT protein expression and consecutive O-GlcNAc activity *in vitro* and *in vivo*. Importantly, we identify O-GlcNAcylation as a crucial mechanism to restore protein maturation − as evidenced e.g. by OGT-dependent externalization of CD45 to the cell surface.

On the cellular level, dronabinol-driven activation of O-GlcNAcylation leads to release of the differentiation blockage of leukemic blasts *in vivo* in two patients treated with dronabinol − whereby the functional role of OGT is confirmed *ex vivo* and in *in vitro* models, including a lentiviral OGT-knock out approach.

Together, we identify O-GlcNAcylation as a crucial mechanism involved in leukemia signal transduction - opening a novel (druggable) field for future leukemia research. Further, these findings will provide the rationale for clinical exploration of dronabinol in acute leukemia.

2. Materials and methods

2.1. Cell lines

The acute T-cell lymphoblastic leukemia cell line Jurkat was obtained from the German Collection of Microorganisms and Cell Cultures (DSMZ). The FLT3 ITD and MLL-AF9 fusion positive acute myelogenous leukemia cell line MOLM14 was kindly provided by Dr. Heinrich, Oregon Health and Science University, Portland, OR.

Cells were cultured in RPMI 1640, supplemented with 10% fetal bovine serum (GIBCO/Invitrogen, Darmstadt, Germany), 1% penicillin G (10,000 units/mL), streptomycin (10,000 μg/mg) and 2 -mmol/L l-glutamine (GIBCO/Invitrogen, Darmstadt, Germany or Biochrom AG, Berlin, Germany). FLT3 ITD was sequence confirmed in MOLM14 cells. Additionally, MOLM14 cells were sensitivityconfirmed in response to a FLT3 inhibitor (sunitinib). Negativity for mycoplasma contamination was confirmed using the pluripotent PCR Mycoplasma test Kit for both cell lines (AppliChem, Darmstadt, Germany).

2.2. Reagents

Dronabinol (i.e. $(-)$-Δ^9-Tetrahydrocannabinol, THC), dissolved in methanol, was obtained from THC Pharm (Frankfurt/Main, Germany) with permission of the Federal Opium Agency at the Federal Institute for Drugs and Medical Device, Germany. Drug-carrier control assays, which did not reveal any significant antileukemic effects at the highest concentration used up to 80 μM, were provided earlier [17]. The selective CB1 antagonist LY320135 and the selective CB2 inverse agonist JTE-907 were purchased from Sigma (St. Louis, MO).

2.3. Isolation of bone marrow and peripheral blood mononuclear cells

Bone marrow aspirate and peripheral blood samples from patients with acute leukemia were collected in 5000 U heparin after informed consent and approval of the ethics committee of the University of Tübingen (188/2018BO2). Mononuclear cells were isolated by Ficoll Hypaque density gradient fractionation [18].

2.4. Whole genome methylation profiling

Genome-wide methylation pattern analyses were performed using either the Infinium HumanMethylation27K [Array #1 (Jurkat cells)] or the HumanMethylation450K [Array #2 (native patient samples)] BeadChip probing > 27,000 respective ~485,000 methylation sites at single-nucleotide resolution. Array #1 targets CpG sites covering over 14,000 genes. Array #2 covers 99% of RefSeq genes, with an average of 17 CpG sites per gene region distributed across the

promoter, 5′UTR, first exon, gene body, and 3′UTR. It covers 96% of CpG islands, with additional coverage in island shores and the regions flanking them. The arrays were set up using standard protocols according to the manufacturer.

In short, Jurkat leukemia cells or native leukemia cells of 5 patients were treated with dronabinol for 12−36 h. Naïve cell samples were used as negative controls. After gDNA isolation and bisulfite conversion, each sample was whole-genome amplified (WGA) and enzymatically fragmented. The bisulfite-converted WGA-DNA samples were purified and applied to the BeadChips. Allele-specific primer annealing was followed by single-base extension using DNP- and Biotin-labeled ddNTPs. DNA methylation values, described as beta values, were recorded for each locus in each sample via BeadStudio software.

Differential methylation analysis can be used to generate a DiffScore that indicates whether or not average Beta values are significantly different across samples. The DiffScore can be generated utilizing an Illumina Custom Model, the Mann-Whitney model, or the T t-test model.

After normalization of the data we calculated the differential expression score by the following equation:

$$deffscore = 10\, sgn(\beta_{cond} - \beta_{ref})\log 10p$$

For a locus with multiple probes, the DiffScores across probes were averaged (and a concordance value between probes reported). In order to assess significance, we used the t-test model with the assumption of equal variance provided by illumina BeadStudio to assess variance across replicate samples.

The experiments were performed in cooperation with the Microarray Facility Tübingen (MFT).

2.5. Immunoblotting

Cell pellets were lysed with 100−150 μL of protein lysis buffer (50 mmol/L Tris, 150 mmol/L NaCl, 1% NP40, 0.25% deoxycholate with added inhibitors aprotinin, AEBSF, leupeptin, pepstatin, sodium orthovanadate, and sodium pyruvate, respectively phosphatase inhibitor cocktails „2" and „1" or „3" (Sigma, St. Louis, MO). Protein from cell lysates (75−200 μg protein) after denaturing was used for whole cell protein analysis by Western immunoblot assays [18] using a BioRad Criterion system (protein separation by SDS-PAGE in 3−8% or 10% polyacrylamide gels followed by electroblotting onto nitrocellulose membranes). Nonspecific binding was blocked by incubating the blots in nonfat dry milk or BSA. Anti-human C/EBPalpha (rabbit), OGT (rabbit), CB1 (goat), CB2 (goat) or Tubulin (mouse) antibodies (Sigma, St. Louis, MO or Cell Signaling Technology, Danvers, MA) were used at a 1:500 to 1:1,000 dilution. Primary antibodies were incubated for one hour or overnight, followed by several washes of Tris-buffered saline (TBS) containing 0.005% Tween 20. Infrared dye-conjugated secondary donkey anti-goat or goat anti-rabbit or anti-mouse antibodies to use in a LI-COR® imaging detection system were used according to standard protocols. Secondary antibodies were applicated for 30', followed by several washes. Antibody-reactive proteins were visualized using a LI-COR Odyssey® fluorescence optical system (LI-COR Biosciences, Lincoln, NE).

2.6. Polymerase Chain Reaction (PCR)

mRNA was isolated and reversely transcribed (RT) using standard techniques following the RNeasy® RNA purification kit (Qiagen, Hilden, Germany). OGT cDNA was amplified and relatively quantified using Roche® LightCycler Technology (Roche, Basel, Switzerland).

2.7. Proteome analysis

Proteins were quantified using the Bradford assay (Bio-Rad, Munich, Germany) and digested by in-solution digestion. Briefly, proteins were reduced with 3 mM dithiothreitol, alkylated with 9 mM iodoacetamide, predigested for three hours with 1:100 (w/w) Lys-C (Wako, Germany) and digested with 1:100 (w/w) trypsin (Promega, USA) for 14 h shaking at room temperature. Before trypsin digestion, samples were diluted with 6 volumes of 50 mM ammonium bicarbonate. Following digestion, samples were acidified using formic acid (FA) to a final concentration of 0.5% (v/v).

Mass spectrometry and data processing: All samples were measured on an EASY-nLC 1200 (Thermo Fisher Scientific) coupled to an Orbitrap Elite mass spectrometer (Thermo Fisher Scientific). Peptides were chromatographically separated using 75 μm (ID), 15 cm packed in-house with reversed-phase ReproSil-Pur 120 C18-AQ 1.9 μm resin (Dr. Maisch GmbH). Peptides were then eluted using a 5−50% of solvent B (80% ACN in 0.1% formic acid) gradient over 213 min. Full-scans were recorded between 300 and 2000 Thompson at a resolution of 120,000 with a target value of 1E6. The top 20 most intense ions from each full scan were selected for fragmentation (MS/MS) by higher-energy collisional dissociation (HCD) using a collision energy of 35% at a target value of 5000 charges. Both MS and MS/MS scans were recorded in the orbitrap. All acquired MS data was processed with the MaxQuant software suite [19] version 1.5.2.8 against the complete Human UniProt database (taxonomy ID 9606) containing 91,646 sequences and a database of 248 frequently observed contaminants. Precursor mass tolerance was set to 6 ppm and 0.5 Da for MS/MS fragment ions. A maximum of two missed cleavages resulting in a minimal length of seven amino acids and full tryptic enzyme specificity were required. OHexNAc, methionine oxidation and protein N-terminal acetylation were defined as variable modifications while carbamidomethylation of cysteines was used as fixed modification. False discovery rate was set to 1% for peptide and protein identifications.

2.8. Short hairpin RNA interference

A short hairpin (sh)RNA approach was established to stably suppress OGT translation. Briefly, a pre-selected individual OGT shRNA construct was cloned into a mammalian GIPZ vector following the trans-lentiviral packaging kit (Dharmacon/Thermo Scientific, MA) and retrovirally transduced into the respective leukemia cell model. An empty vector was used as a negative control. Puromycin selection was performed to establish stably expressing OGTi cell strains.

2.9. Apoptosis assays

An annexin V/propidium iodide-based assay was established (Immunotech, Marseilles, France): Translocation of phosphatidylserine from the inner to the outer leaflet of the plasma membrane as an early indicator of apoptosis (annexin V positivity) and permeability of the cell membrane as a sign of late phase apoptosis or dead cells (propidium iodide stain of DNA) was measured using a FACScalibur® flow cytometer loaded with CellQuest® analysis software (BD, Heidelberg, Germany) [18].

2.10. Immunophenotyping

Extracellular expression of CD11c, CD13, CD14, CD15 and CD34 was assayed using standard protocols for PE-, FITC- or APC- conjugated antibodies. Cells were acquired on a FACScalibur® flow cytometer and analyzed using the CellQuest® software.

In brief, antibodies were added in a 1:20 dilution to the cell suspension and incubated for 1 h at room temperature followed by PBS washing and resuspension. After rinsing and resuspension, cells were assayed using a FACScalibur® flow cytometer and CellQuest® analysis software.

2.11. Intracellular protein expression

Cells were fixed and permeabilized using the Fix and Perm Fixation and Permeabilization kit (ADG An der Grub Bioresearch, Kaumberg, Austria). Unconjugated primary OGT antibody (Signaling Technology, Danvers, MA) was added in a 1:20 dilution to the cell suspension and incubated for 1 h at room temperature followed by PBS washing and resuspension. Fluorescent dye-conjugated (AlexaFluor) secondary goat anti-rabbit was added in a 1:50 dilution and cells were incubated for 30 min at room temperature. After rinsing and resuspension, OGT-protein expression levels were assayed using a FACScalibur® flow cytometer loaded with CellQuest analysis software (BD, Heidelberg, Germany).

2.12. Image stream multispectral imaging cytometry

Multispectral imaging flow cytometry combines the features of fluorescence microscopy and conventional flow cytometry and enables a discrimination of cells objectively and statistically based on their appearance.

For each sample, images of at least 5.000 cells were acquired on the ImageStream^X mkII with the INSPIRE instrument controller software (Merckmillipore/amnis, USA). Cells were collected with 40x magnification and the 488 nm laser power set to 20 mW and the 561 nm laser power set to 100 mW.

Data was analyzed with IDEAS® Image analysis software. Median CD45-PE fluorescence intensity was analyzed in all single cells in focus.

2.13. Cytomorphology

A May-Gruenwald-Giemsa staining protocol was set up to analyze patients` blood smears on a confocal Zeiss® AXIO Imager.A1 microscope (Carl Zeiss AG, Goettingen, Germany).

2.14. Cell sort and mutation analysis

The CDKN2A mutation, which was followed in the cell sort experiments for the T-ALL patient, was initially identified in a next generation amplicon based deep sequencing (NGS) approach: Targeted multigene mutation screening was performed by NGS on an Ion Torrent PGM (Thermo Fisher Scientific, Waltham, MA, USA) using the AmpliSeq Cancer Hotspot Panel v2 (hotspot regions in 50 genes: ABL1, EZH2, JAK3, PTEN, AKT1, FBXW7, IDH2, PTPN11, ALK, FGFR1, KDR, RB1, APC, FGFR2, KIT, RET, ATM, FGFR3, KRAS, SMAD4, BRAF, FLT3, MET, SMARCB1, CDH1, GNA11, MLH1, SMO, CDKN2A, GNAS, MPL, SRC, CSF1R, GNAQ, NOTCH1, STK11, CTNNB1, HNF1A, NPM1, TP53, EGFR, HRAS, NRAS, VHL, ERBB2, IDH1, PDGFRA, ERBB4, JAK2, PIK3CA). Amplicon library preparation and semiconductor sequencing was done according to the manufacturers' manuals using the Ion AmpliSeq Library Kit v2.0, the Ion PGM^{TM} Hi-Q^{TM} OT2 Kit and the Ion PGM^{TM} Hi-Q^{TM} Sequencing Kit (Thermo Fisher Scientific).

Detection of non-synonymous variants compared to the human reference sequence was performed using Ion Torrent Variant Caller. Detection thresholds were set at an allele frequency of 5%. Variants were annotated and filtered against the dbSNP and COSMIC databases using the annotate variants single sample workflow of the Ion Reporter Software (Thermo Fisher Scientific).

Cell sort and CDKN2A mutation screen (T-ALL patient): Cells were sorted according to cell size (FSC scatter) and granularity (SSC scatter), harvested and proceeded to mutation analysis following Sanger sequencing. Genomic DNA was isolated from sorted cells using the Maxwell(R) 16 Blood DNA Purification Kit (Promega, Mannheim, Germany). To detect the nonsense mutation p.R80* (c.238C>T), DNA was amplified for exon 2 of the CDKN2A gene using M13-tailed primers: forward 5'-TGTAAAACGACGGCCAGTCTTCCTTTCCGTCATGCCG-3',

reverse 5'-CAGGAAACAGCTATGACCAG GTACCGTGCGACATC-3'. PCR was performed using 20 ng DNA template in a final volume of 25 μl with 0.2 μM of each primer, 0.2 mM dNTPs, 1.5 mM MgCl2 and 0.5 Units Phusion HotStart High Fidelity Polymerase (Finnzymes, Woburn, MA, USA). Cycling conditions entailed an initial denaturation at 98 °C for 30 s followed by 45 cycles of denaturation (98 °C for 10 s), annealing (56 °C for 45 s) and elongation (72 °C for 30 s), with a final elongation at 72 °C for 4 min.

PCR products were purified (AMPure, Beckman Coulter, Brea, CA, USA) and aliquots of 7 μl were used for the sequencing reaction with 1 μM of the universal M13 sequencing primer and 2 μl of GenomeLab DTCS-Quick Start Kit (Beckman Coulter, Brea, CA, USA) in a final volume of 10 μl according to the manufacturers protocol. Sequencing reactions were purified (CleanSEQ, Beckman Coulter, Brea, CA, USA) and analyzed in a GenomeLab GeXP Genetic Analysis System and evaluated by the GenomeLab GeXP software 10.2 (Beckman Coulter, Brea, CA, USA) to determine the mutation status.

Cell sort and mutation screen (AML patient): Cells were sorted according to multi-color stain of PE-conjugates of CD34, CD117, CD135 and CD133 and with CD14-FITC. To exclude leukemia contamination (e.g. in the lymphocyte cohort) the initial leukemia clone was identified in a co-stain for CD34+CD117+CD133+CD135+.

For mutation analysis several strategies were followed: 1st gDNA Sanger sequencing [on ABI3730] of a 27 gene panel, [Exons in brackets: ASXL1 [12]; BRAF [15]; CALR [9]; CBL [8,9]; CEBPA [1]; CSF3R [13−17]; DNMT3A [8,9,12−23]; ETV6 [1−8]; EZH2 [2−20]; FLT3 (14-15 ITD, 20); IDH1 [4]; IDH2 [4]; KRAS [2,3]; NPM1 [12]; NRAS [2,3]; PHF6 [2−10]; PTPN11 [3]; RUNX1 [1−8]; SETBP1 (distal 34); SF3B1 [12−16]; SH2B3 (distal 3'-2); SRSF2 [1]; TET2 [3−11]; TP53 [4−9]; U2AF1 (2,6, syn. U2AF35); WT1 [7,9]; ZRSR2 [2−11], 2nd additional cDNA Sanger sequencing of a 3 gene panel [JAK2 [12−15]; KIT [8−17]; MPL [10−11] and 3rd complementary next generation amplicon based deep sequencing (NGS) using a myeloid gene panel (NGHS-013X, Qiagen; 2826 amplicons; complete coding sequence of ABL1, ASXL1, ATRX, BCOR, BCORL1, CBL, CBLB, DAXX, DNMT3A, EED, ETV6, EZH2, FLT3, GATA1, GNAS, IDH1, IDH2, IKZF1, JAK1, JAK2, JAK3, KAT6A (MYST3), KIT (CD117), KRAS, MLL, MPL, NF1, NPM1, NRAS, PHF6, PRPF40B, PTPN11, RAD21, RB1, RUNX1 (AML1), SETBP1, SF1, SF3A1, SF3B1, SH2B3, SMC1A (SMC1L1), SMC3, STAG2, SUZ12, TET2, TP53, U2AF1, U2AF2, WT1, ZRSR2) on Illumina Myseq platform following the providers´ instructions for amplicon generation and library preparation with Illumina TruSeq technology and MiSeq v3 reagents for a 2 × 125 cycles run.

All mutations found with NGS were confirmed with Sanger sequencing. The primers of this confirmative approach were also used to check sorted monocyte, lymphocyte and progenitor patient sample cohorts DNA for presence of mutations found in unseparated leukocyte DNA.

To prove a supposed EZH2 deletion and test for the extent of loss of chromosome 7, multiplex ligation-dependent probe amplification (MLPA) was employed following the suppliers instructions with a slight modification due to low DNA concentration of sorted cells (5 additional cycles PCR; MRC-Holland, MDS Kit P414-A, ABI-3730).

2.15. Cytogenetics

Chromosomal analysis of mononuclear cells was performed after Ficoll Hypaque density gradient fractionation according to standard protocols. After GTG-banding 54 mitoses were structurally analyzed.

2.16. Plasma inhibitory assay (PIA)

PIA was set up using a modified method described by Levis and colleagues [20]: the patient's plasma was harvested while on treatment with dronabinol 2,5% (6 drops BID) and used to culture a control cell line (Jurkat) for 48 h. Induction of apoptosis was evaluated in an annexin V-based assay.

2.16. Statistical analysis

Samples were compared primarily using one-way ANOVA. In the case of a statistically significant one-way ANOVA result, Tukey's honestly significant difference (HSD) test and Dunnett's test for comparison with a single control, were performed as post hoc tests, respectively. Test results yielding a P value less than 0.05 were assumed to indicate statistical significance. This part of the analysis was done with the JMP® 11.0 statistical software (SAS Institute, Cary, NC, USA).

2.17. Data and materials availability

Array data were deposited in the PRIDE database:

Project Name: Epigenetic activation of O-linked βN-acetylglucosamine transferase overrides the differentiation blockage in acute leukemia.
Project accession: PXD017302

3. Results

3.1. Release of the differentiation block upon dronabinol in a patient with T-Lymphoblastic lymphoma/leukemia in vivo

We present a 21-year old male patient, suffering from highly aggressive T-lymphoblastic lymphoma, with leukemic relapse after allogeneic bone marrow transplantation and refractory disease after salvage chemotherapy.

Cytoreductive therapy with dexamethasone was initiated (d−1 − d+3) (see supplemental table S1 for cell counts and therapy schedule). Supportive care treatment included dronabinol 2,5% oily solution (starting with 3° BID on day 0 and tampered to 6° TID) to comfort the patient's well-being with regard to inappetite and beginning of cachexia.

Using a peripheral blood sample of this patient taken at diagnosis of relapse, potent *ex vivo* cytoreductive sensitivity towards dronabinol was noted (supplemental Fig. S1a). Further, surprisingly, on day 15 morphologically differentiating cells were observed (Fig. 1a). A cell sort was set up to analyze the suspected cohorts for the presence of a CDKN2A C238T mutation, which had been described in the lymphoblastic leukemic cohort at relapse (NGS targeted multigen screen, not shown, methodology described in methods).

Intriguingly, the mutant CDKN2A C238T isoform was detected not only in the lymphoblastoid population (cohort 1) as expected − but also in the differentiating cohorts (cohorts 2/3), (Fig. 1b−d). Of note, allele frequency of mutant-CDKN2A in cohort 3 was 35% as validated by NGS, which accounts for presence of mutated CDKN2A in 70% of cells of the targeted population, ruling out contamination after cell sort and false positive detection of mutant-CDKN2A by Sanger sequencing.

Thus, molecular finger printing highly suggests that dronabinol has contributed to the release of the differentiation block in this patient.

3.2. Dronabinol modulates gDNA methylation

To mimic a potential differentiating effect of dronabinol we next used the Jurkat cell line to elaborate this hypothesis: We speculated, that cellular differentiation is driven via a so far unknown, epigenetic capacity of dronabinol. A gene-chip gDNA methylation screen was set up using our well-established dronabinol sensitive T-lymphoblastic Jurkat leukemia model [17]. Cells were exposed to dronabinol (20 μM) for 12 h and 32 h and probed for changes in methylation patterns throughout the genome (see also methods section for a more detailed description of the array).

Dronabinol proved to modulate gDNA methylation in a time-dependent manner. Significant changes of methylation patterns, which were defined as a $\geq$10% change in methylation, affected 120 probes after 12 h and 347 probes after 32 h post treatment with dronabinol. Hypomethylation was thereby more prevalent (71 probes after 12 h / 285 probes after 32 h) compared to gain of methylation (49 probes after 12 h / 62 probes after 32 h) (Fig. 2a/c).

Dronabinol affected methylation of a multitude of genes encoding for proteins orchestrating diverse functions, including transcription factors and epigenetic regulators, chemokines or cytokines and kinases. Supplemental Table S2 provides the entire list of significantly altered probes and linked genes. The top five highest scoring genes with regard to hypo- or hypermethylation after exposure to dronabinol are provided with Fig. 2b/d.

3.3. Time-dependent hypomethylation of O-linked N-acetylglucosamine (O-GlcNAc) transferase (OGT) upon dronabinol exposure

Next, we focused our studies on the highest altered probe, displaying a decrease in methylation of −42% with a p-value of 3,68E−38 (from a basal methylation level of 68%) 32 h after treatment: This probe (ID cg26399113, mapping on the X chromosome on position 70,669,364) locates to the transcription factor binding site of the O-linked N-acetylglucosamine (O-GlcNAc) transferase (OGT). Hypomethylation of this site is likely to link to initiation of transcription [21].

In accordance to profound time-dependent hypomethylation of the OGT gene, we confirmed time-dependent increase of OGT protein expression levels in Jurkat cells by Western immunoblotting − peaking 36−48 h after administration of dronabinol (Fig. 3a). In concordance, upregulation of OGT protein expression went along with elevated mRNA transcript levels (Fig. 3b).

Notably and in concordance with the findings in Jurkat T-lymphoblastic leukemia cells, increase of OGT expression levels in response to dronabinol was validated *ex vivo* in a sample of the reported patient (supplemental Fig. S1b).

To test whether upregulation of OGT protein expression levels translates into increased transferase activity, whole cell extracts derived from Jurkats exposed to dronabinol were immunoblotted for O-GlcNAcetylation of serine/threonine residues. Fig. 3c demonstrates a significant increase of O-GlcNAcetylation affecting several proteins upon treatment with dronabinol.

Following a MaxQuant-based mass spectrometry approach, we identified 125 peptides with localized O-glycosylation sites (entire list provided in supplemental Table S4). The top 20 scoring GlcNac sites involve proteins associated with signal transduction (PKCB1, PPIP5K2, PTPRC), cell repair (NBN), transcription regulation (ZMYMD8, NACC1, ZBED6, ZNF71) or iron uptake (TFR1) (Fig. 3d).

It is utmost noteworthy, that Protein tyrosine phosphatase receptor type C (PTPRC, i.e. CD45), is tightly linked with hematopoiesis and leukemia: The CD45 phosphatase is expressed on all nucleated hematopoietic cells and plays a central role in cell growth and differentiation, which is best studied in lymphocyte development and antigen receptor signaling (reviewed by Hermiston, Xu and Weiss [22]. Thereby, mature CD45 is heavily glycosylated, which is required for cell surface expression [23].

In contrast, leukemic blasts typically display only moderate CD45 expression levels [24,25], indicating blockage of cellular maturation. Hypothetically, restoration of CD45 expression may contribute to release of the differentiation blockage observed in acute leukemia.

Consequently, we used our Jurkat cell model − and indeed demonstrate increase of CD45 expression levels at the cell surface upon exposure towards dronabinol, as indicated by single-cell image stream flow cytometry (Fig. 3e−g).
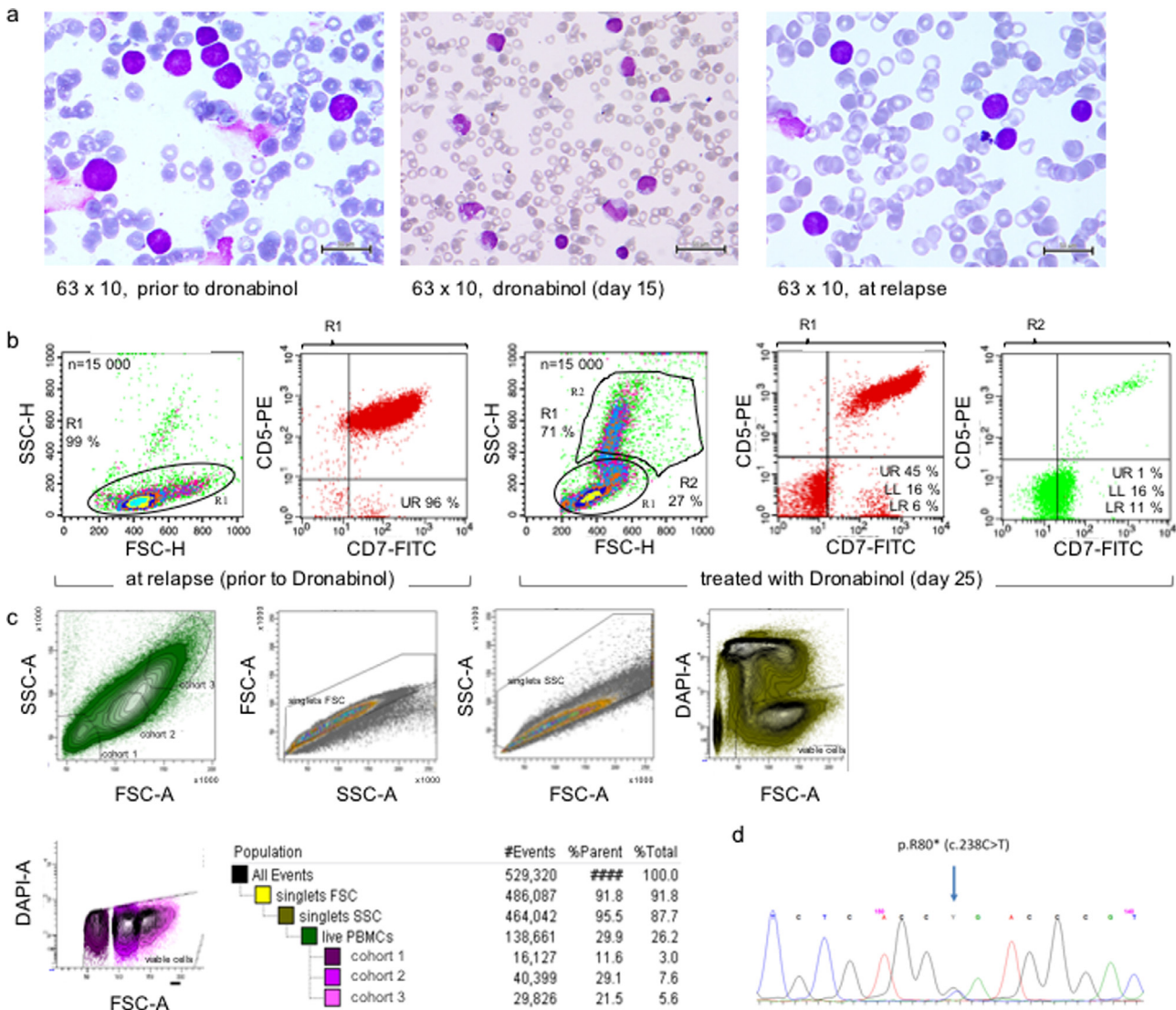
Fig.1. Dronabinol induces differentiation of the leukemic clone in a patient with relapsed T-lymphoblastic leukemia *in vivo*. (a) Course of disease (refer also to supplemental Table S1), cytomorphology: May-Gruenwald-Giemsa stain at relapse, prior to dronabinol (left panel), 15 days after start of treatment with dronabinol (mid panel) and at reoccurrence of disease after salvage chemotherapy (right panel). (b) Course of disease, immunophenotype: Immunophenotype prior to and under therapy with dronabinol. (c) Cell sort of T-ALL patient sample with suspected maturation (cohort 2/3) of leukemia blasts. (d) Representative electropherogram of the CDKN2A p.R80* (c.238C>T) mutation detected in all cohorts.

3.4. Validation of epigenetic activity of dronabinol in an independent methylation array using native leukemia cells

To validate the methylation data obtained for the Jurkat cell line *in vitro*, we set up an independent gDNA methylation array screen using *native* acute leukemia blasts. Five acute lymphoblastic and myeloid leukemia patient samples with confirmed proapoptotic sensitivity towards dronabinol [17] and Jurkat cells serving as reference control, were treated with sub-IC50 doses of dronabinol (20 mM) for 24 h and gDNA was isolated and probed after bisulfite conversion in an independent Ilumina Infinium methylation array. Principal component analysis (PCA) comparing dronabinol-exposed with drug-naive samples revealed similarly directed shifts of methylation patterns in all cases – with high interindividual variances of absolute values (Fig. 3h).

However, concentrating on probes located within the *OGT* gene region, we verified a distinct shift towards CpG hypomethylation of two probes at the transcription start site (TSS) (Fig. 3i), an additional heatmap is provided as supplemental Fig. S2. Statistical comparison to all other probes confirmed significance for both probes (Fig. 3j/k). Intriguingly, the highest altered probe (Fig. 3k) at TSS1500 (ID

cg26399113) corresponds to the probe altered in the Jurkat methylation array – confirming the observation made for the Jurkat cell line.

It has to be noted, that the hypomethylating effect (after 24 h of exposure to dronabinol) was not as pronounced compared to the initial Jurkat methylation array (measured after 32 h). However, this observation is in concordance with our Western immunoblot assays (compare Fig. 3a) arguing for a time-dependent increase of OGT protein expression levels peaking at 36 h after administration of dronabinol.

For further validation, patient samples used in the methylation screen were treated with dronabinol for 24 h with 20 μM or 40 μM and OGT protein expression was assessed by FACS flow cytometry applying an intracellular protein staining protocol. Indeed, a statistically significant increase of OGT protein expression levels was demonstrated (Fig. 3l).

3.5. OGT-interference results in decreased susceptibility towards induction of apoptosis

Due to the impact of dronabinol on gDNA methylation patterns of hundreds of genes, a putative passenger role of OGT versus distinct antileukemic efficacy was ruled out:
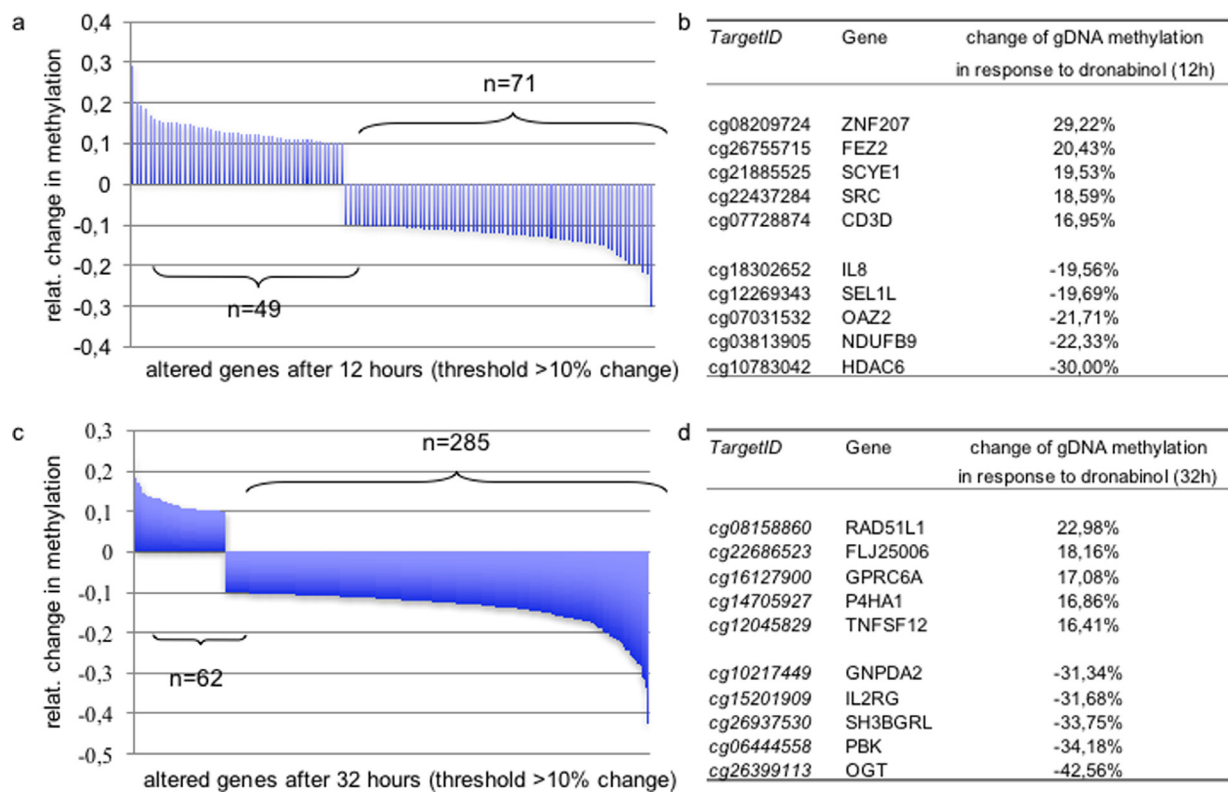
Fig. 2. Change of gDNA Methylation of Jurkat leukemia cells in response to dronabinol. Waterfall plots of probes demonstrating change of methylation levels in a gDNA methylation array after 12 h (a) or 32 h (c) of exposure to dronabinol (20 μM). Threshold +/- ≥ 10%. (b) Ranking of top-5 highest scoring altered genes after 12 h (b) or 32 h (d) of treatment. A detailed list of all significantly altered genes is provided as supplemental Table S2. Experiments performed in technical triplicates.

Stable OGT knock-down Jurkat strains were generated using a lentiviral shRNA transduction approach. Transduction efficiency of the GIPZ plasmid vector (encoding a green fluorescent protein detection control) was demonstrated by flow cytometry (Fig. 4a). Consecutively, successful suppression of OGT protein expression in comparison to the parental cell line and an empty vector control strain was confirmed in a Western immunoblot (Fig. 4b).

OGT-interferenced (OGTi) cells were next treated with dronabinol in dose-dilution series and induction of apoptosis was measured in an annexin V-based assay. Indeed, proapoptotic efficacy of dronabinol was demonstrated – whereas concentrations to reach >IC50s are rather high. OGTi cells were thereby statistically significantly less susceptible to the proapoptotic effect of dronabinol compared to the empty vector control cells ($p = 0.02$) (Fig. 4c).

3.6. Validation of OGT- dependency in native leukemia cells

Next, native patient samples used in the methylation array were retrovirally transduced with an OGT shRNA GIPZ vector construct. Successful transduction was confirmed after 48 h flow cytometrically via verification of GFP positivity (Fig. 4d) and cells were then treated for another 48 h with dronabinol in dose dilution series.

Reduction of viable GFP-positive mononuclear cells was analyzed by flow cytometry using a FSC/SCC scatter plot (method described recently [17]). Again, OGTi-cells were significantly less susceptible towards dronabinol with only moderate reduction of the viable cell fraction in a concentration killing approx. 70% of cells transduced with an empty vector control ($p = 0.01$) (Fig. 4e).

These observations strongly suggest direct implication of OGT in proapoptotic pathways in acute leukemia cells exposed to dronabinol *in vitro* and *ex vivo*.

### 3.7. Dronabinol induces cellular differentiation in Jurkat leukemia cells in an OGT-dependent manner

As we have demonstrated, dronabinol may exert cellular differentiation of leukemia cells (compare Fig. 1a). To (a) confirm the differentiation capacity of dronabinol and (b) evaluate, whether dronabinol-mediated effects on cellular differentiation depend on OGT, we used the T-lymphoblastic OGTi-Jurkat model to assess for CD11c expression levels:

Expression of CD11c, a subunit of a heterodimeric integrin receptor which is expressed in many mature leukocytes including dendritic cells, monocytes, neutrophils, B-cell subsets (summarized by Stewart et al. [26]) – but also in activated T-cells [27,28], was used as a marker for maturation and assessed flow cytometrically.

Whereas induction of apoptosis was predominant in the highest doses (compare Fig. 4c), treatment with sub-IC50 concentrations of dronabinol retained a viable population – which was followed for signs of maturation 72 h after exposure. Upregulation of CD11c was noted in the Jurkat empty vector control strains – arguing for release of the differentiation blockage and maturation of cells. In contrast, no significant increase of CD11c expression was observed in OGT-interferenced cells (Fig. 5a/b, carrier control provided with supplemental Fig. S6b).

In addition, dronabinol had no impact on CD45 expression in *OGT* knocked-down Jurkat cell strains as well (Fig. 5c), validating O-GlcNAc-dependency of cellular maturation processes (compare Fig. 3e−g).

To further validate the role of O-GlcNAcylation as an important mechanism to induce cellular differentiation in leukemia blasts, we followed a dronabinol-independent approach: O-GlcNAcylation is physiologically reversed by O-GlcNAcase (OGA) – and inhibition of OGA results in increased GlcNAcylation of serine and threonine
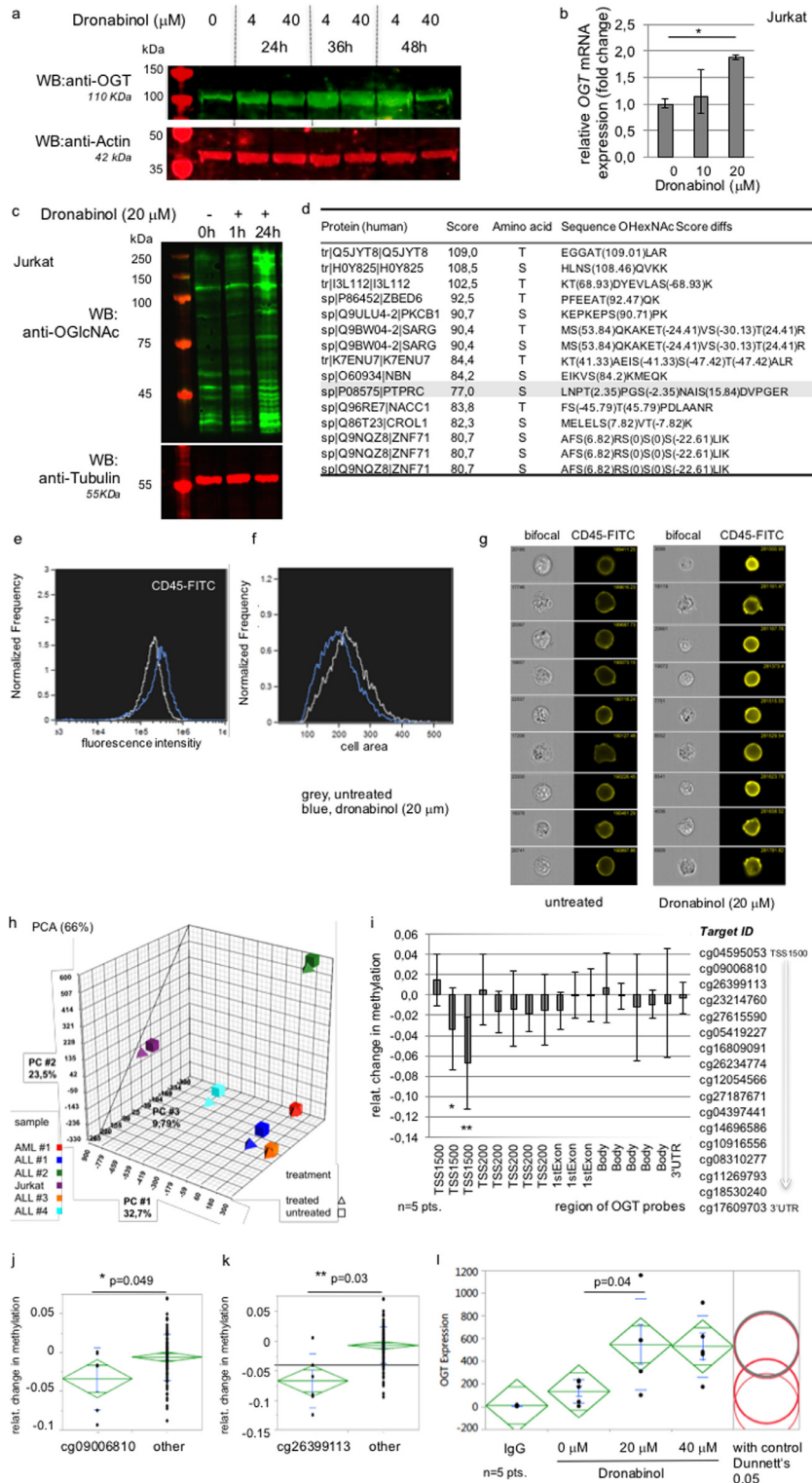
Fig. 3. Dronabinol induces expression of O-linked N-acetylglucosamine transferase (OGT). (a) Representative Western immunoblot of Jurkat cells treated with dronabinol. Probing for Actin serves as loading control. First lane: protein ladder. (b) qRT-PCR of Jurkat cells treated with dronabinol. Relative fold change of OGT expression levels are shown. * confidence interval 95%. GAPDH serves as housekeeping gene. (c) Representative Western immunoblot of Jurkat cells demonstrating O-GlcNAcylation upon exposure to dronabinol. First lane: protein ladder. (d) Ranking of top-15 highest scored altered peptides identified by MaxQuant-based mass spectrometry. (e-g) Image stream multispectral imaging cytometry demonstrates upregulation of CD45 at the cell surface upon exposure to dronabinol of Jurkat cells in a single cell approach. (f) Note that maturing cells trend to a decrease in size. (h) Principal Component Analysis (PCA) of an InfiniumMethylation450K array using 5 patient samples with AML or ALL or Jurkat cells treated with dronabinol (24h) vs. an untreated control. (i) Relative change of methylation levels of probes linking to the OGT region. TSS (transcription start site), 3'UTR (untranslated region). A heatmap is provided with supplemental figure S2. (j/k) Statistical proof of significance of demethylation of two probes within TSS1500 compared to all other probes. Statistical significance at $p < 0.05$ (one way ANOVA). (l) Intracellular stain of OGT expression levels upon dronabinol exposure for 24 h in the respective native acute leukemia samples. Geometric mean as assessed by flow cytometry is shown. Statistical significance at $p < 0.05$ (one way ANOVA), with control (Dunnett's test).
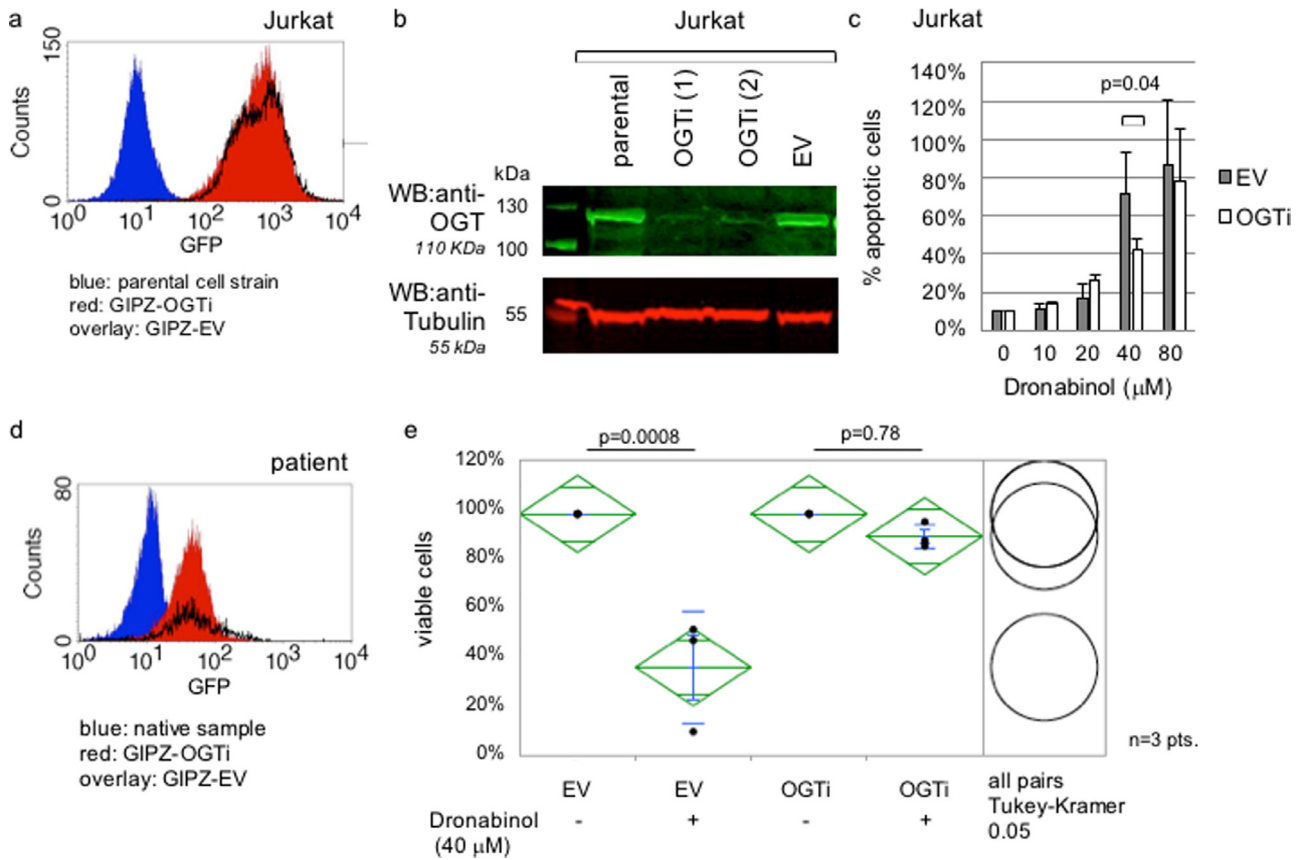
Fig. 4. **Suppression of OGT in Jurkat leukemia cells using an shRNA approach.** (a) Representative flow cytometry assay to determine transduction efficiency as assessed by green fluorescence protein (GFP) reactivity. GIPZ-OGTi (lentiviral plasmid OGT shRNA vector), EV (empty vector control). (b) Representative western immunoblot demonstrating successful suppression of OGT translation in two strains (OGTi(1/2)). EV (empty vector control). Probing for tubulin serves as loading control. (c) Annexin V/propidium iodide-based flow cytometry assay to determine induction of apoptotis in response to dronabinol (culture time 48 h). OGTi (OGT-interference), EV (empty vector control). Statistical significance at $p < 0.05$ (one-way ANOVA). (d) Suppression of OGT expression in native leukemia blasts as determined by flow cytometry: transduction efficiency assessed by GFP reactivity. GIPZ-OGTi (lentiviral plasmid OGT shRNA vector), EV (empty vector control). (e) A FSC/SSC-based flow cytometry assay to determine the viable population after treatment with dronabinol for 48 h. Pts (native acute leukemia patient samples), OGTi (OGT-interferenced patient samples), EV (empty vector control). Statistical significance at $p < 0.05$ (one-way ANOVA), with all pairs (Tukey-Kramer), $n = 3$ pts.

residues of respective target proteins [29]. A potent OGA-selective inhibitor, Thiamet-G (TMG), was used to address whether OGA inhibition results in a release of the differentiation blockage in leukemia cells. We demonstrate that TMG is capable to increase PTPRC/CD45 protein levels in Jurkat cells as assessed by flow cytometry (Fig. 5d), again arguing for a substantial role of O-GlcNAcylation on cellular maturation to override the cellular differentiation blockage in leukemia cells.

3.8. Confirmation of OGT-dependent antileukemic efficacy of dronabinol in a leukemia patient with secondary (s)AML

3.8.1. Case report

A 90 year old patient with a history of a 4-x aortocoronary bypass, was admitted to the hospital with cardiac decompensation as well as pneumonia superimposed on pulmonary edema. Rapidly rising leukocytes and bleeding complications due to thrombocytopenia lead to referral to the hematology department, and acute myeloid leukemia with ~80% leukemic blasts in the peripheral blood was diagnosed. White blood cell count peaked at $103\,000/\mu l$. Due to multimorbidity, bone marrow biopsy was not performed. Immunophenotyping displayed immature CD34+/HLA-DR+/CD13+/CD33+/CDw65+/MPO positive myeloid blasts. Lymphoid markers were not expressed. A marginal subpopulation showed myelomonocytic differentiation with CD14+/CD15+ positivity. Documented patient's history of unilineary myelodysplasia with transfusion independent macrocytic anemia tracking back to 2007 argues for diagnosis of sAML with myelodysplasia-related changes [30].

Initial cytoreductive treatment using hydroxyurea (HU, $2-3 \times 1g$) resulted in a steady decrease of the white blood cell count (WBC, Fig. 6 and supplemental table S5). HU was tampered ($1 \times 1,5g$) with declining WBC and then halted.

However, blasts rapidly recovered — and despite restart of HU ($2 \times 1g$ at WBC $8720/\mu l$) dynamic disease with doubled leukocytes was noted the next day (WBC $19\,460/\mu l$).

To comfort the patient's well-being with regard to nausea and stimulation of appetite and on the basis of our *in vitro* data demonstrating a potential effect of THC in acute leukemia [17] a compassionate use attempt with dronabinol 2,5% oily solution was started and titrated dropwise according to tolerability to a maximum dose of 6 drops BID. Leukocytosis ceased, followed by a decrease of WBC into the subnormal range. HU was stopped, whereas dronabinol was retained at 6 drops BID. Intriguingly, blasts subsided in the peripheral blood — going along with regeneration of neutrophils and platelets into the normal range.

Due to neutropenic pulmonary infection one shot of G-CSF 30 MioE was administered once (d32). No further specific antileukemic treatment or growth factor support was administered further on.

The patient recovered from pneumonia and recompensated with cardial function — and was discharged to home care. Following up, convalescence of clinical conditions to a normal age-adapted ECOG performance status was reported two months after first diagnosis of AML.
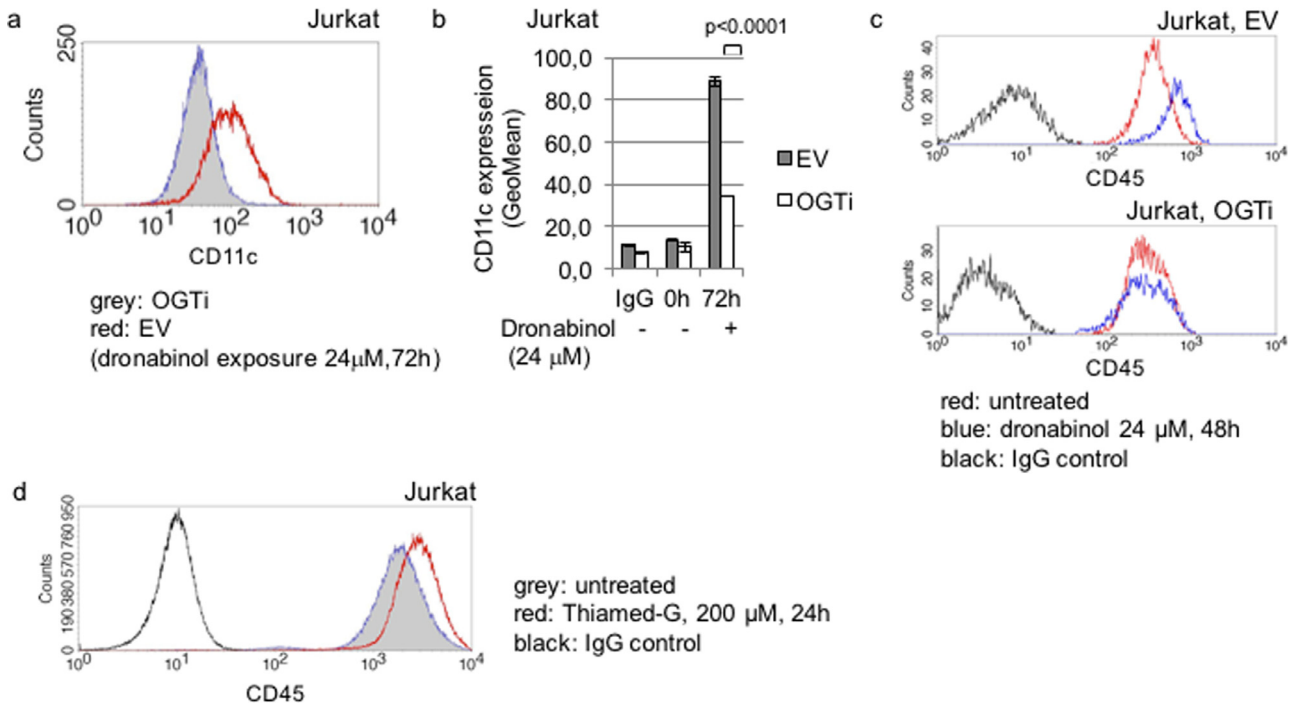
Fig. 5. Release of the differentiation blockage upon dronabinol in Jurkat leukemia cells. (a) Representative flow cytometry histogram of relative CD11c expression of OGT-inter-ferenced (OGTi) Jurkat cells in response to dronabinol compared to an empty vector (EV) control strain. (b) Summary of three independent measurements of CD11c expression levels. Statistical significance at $p < 0.05$ (one-way ANOVA). (c) Representative measurement of CD45 expression in OGT-interferenced (OGTi) Jurkat cells exposed to dronabinol, compared to the empty vector (EV) cell strains. (d) Representative graph of relative CD45 expression levels of Jurkat cells treated with the OGA inhibitor Thiamed-G.
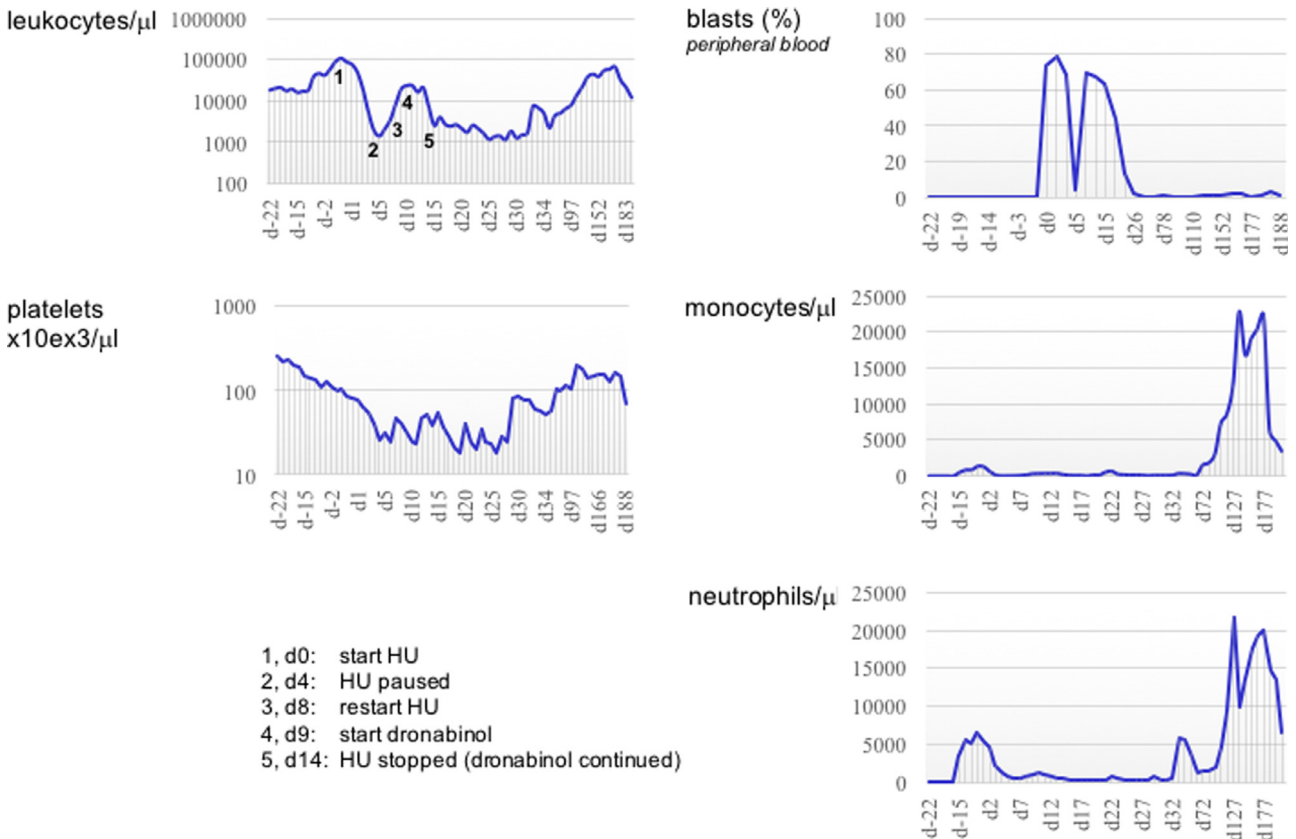
Fig. 6. Course of disease in an AML patient treated with dronabinol. Peripheral blood counts from admission to hospital until lost-to follow up. Absolute blood counts are pro-vided with supplemental Table S5.

Remission with cytomorphologically mature granulocytes, virtual absence of blasts and normalized platelets was stably documented. Notably, an increase of granulocytes and monocytoid cells was observed around day 100 on dronabinol treatment. Due to continuing increase of leukocytes – in the absence of blasts – HU cytoreduction was initiated (d169). Platelets remained in the normal range and cytology indicated maturing cells, suggestive of differentiation of the leukemic clone.

About half a year into therapy with dronabinol the patient resuffered cardiac decompensation and refused any further therapy – and was lost to follow up.

3.9. Molecular validation of dronabinol-driven antileukemic activity

Due to this extraordinary course of disease, we speculated that dronabinol exerted direct antileukemic activity in vivo.

We first determined whether the patient's blasts express the cannabinoid receptors CB1 or CB2. Western immunoblotting of protein lysates derived from peripheral blood mononuclear cell (PBMC) extracts at diagnosis demonstrated high expression levels for CB1 as well as CB2 comparable to a positive control cell line (Jurkat T-lymphoblastic leukemia cell line [17]) (Fig. 7a).

Next, ex vivo cytotoxic sensitivity towards dronabinol was determined in a Ficoll-isolated mononuclear cell sample of this patient from time of diagnosis, cultured and treated with dronabinol in serial dilutions for 48 h. Efficacy was assessed flow cytometrically (Fig. 7b) – with IC50s in the range of previous data for native AML patient samples [17].

To address, whether effective concentrations of dronabinol are achievable in vivo, a plasma inhibitory assay was set up using patient's plasma harvested while on treatment with dronabinol 2,5% (6 drops BID) to culture a control cell line (Jurkat) for 48 h. Induction of apoptosis was documented in an annexin V-based assay, indicating potent plasma inhibitory efficacy (Fig. 7c).

Importantly, an increasing monocyte and neutrophil population was observed the following months. Cytomorphology demonstrated dysplastic but differentiating monocytes and granulocytes (Fig. 7d). In line, immunophenotyping revealed loss of CD34 expression while maintaining/increasing monocytic and granulocytic markers – indicating maturation of the leukemic clone (Fig. 7e).

To validate differentiation of the leukemic blasts, we mimicked this effect ex vivo: a sample of this patient taken at diagnosis was treated with dronabinol at sub-IC50 concentrations (24 μM). And indeed, in analogy to the in vivo observations in this patient, maturation of leukemic blasts upon dronabinol exposure was demonstrated ex vivo, as indicated morphologically by a shift to larger and more granulated cells (Fig. 7f) as well as by relative upregulation of granulocyte and monocyte maturation markers (CD11c, CD14 and CD15) and profound decrease of the CD34 progenitor cell marker (Fig. 7g).

To trace back the origin of the differentiated monocytic and granulocytic populations in this patient, a molecular screen was set up: Patient samples of unseparated leukocytes taken at diagnosis and 4 months after start of treatment with dronabinol were prepared for next generation amplicon based deep sequencing (NGS) using a myeloid gene panel of 55 candidate genes. In parallel Sanger sequencing was performed to confirm gene mutations of interest.

The Illumina NGS run for that sample yielded 4.3 Mio reads with a total of 1 gigabases, whereof 95.8% had a quality score exceeding Q30, resulting in an average coverage of 8025. Together, a total of 5 somatic mutations in 4 genes known to be linked with acute leukemia were identified, including Enhancer of zeste homolog 2 (EZH2_c.434T>C for p.Phe145Ser), Additional Sex Combs Like Transcriptional Regulator 1 (ASXL1_c.1903G>T for p.Glu635*), Neurofibromin 1 (NF1_c.3527_3528insAGCT for p.Thr1178Serfs*18 and NF1_c.375delT for p.Glu126Lysfs*39) and Fms-Related Tyrosine Kinase 3 (FLT3_c.2028C>A for p.Asn676Lys) [1,31,32]. Additionally, a

striking 90 to 10 ratio for major and minor allele at a SNP in EZH2 [rs2302427] pointed to loss of heterozygosity (LOH), which was confirmed by multiplex ligation-dependent probe amplification (MLPA) (Fig. 8a).

Next, we aimed to delineate wether the detected mutations associate with specific leukocyte populations. To succeed with this aim a cell sort was set up using patient samples taken two months after start of treatment. The sorted cohorts include a granulocyte population (CD15+/CD34-; isolated from a whole cell blood sample), a mature monocytoid population ("P6", CD14+/CD34-/CD135-/CD117-/CD133-), a lymphocyte population ("P4", confirmed negativity for CD14/CD34/CD135/CD117/CD133 defining the leukemia clone), a residual monoblast-like progenitor cell population ("P5", CD14+/CD34+/CD135+/CD117+/CD133+), and a residual (myeloblast-like) progenitor cell population ("P7", CD34+/CD14-/CD135+/CD117+/CD133+); ("P4-7" were sorted from mononuclear cells) (supplemental Figs. S3 and S4). Consecutively, a mutation search was performed on each cohort. Results are depicted in supplemental table S6.

Taken together, the findings from the mutation screen prove that the differing phenotypes originate back to one (pre)leukemic clone evolving from an EZH2 SNP, which was also heterozygously detected in lymphocytes (Fig. 8c). Molecular evolution then led to segregation of two major subclones: the first clone harboring a FLT3 and an additional EZH2 pointmutation – and a second clone with a monocytoid phenotype with acquired monosomy 7 and additional ASXL1 and NF1 mutations, further separating subclones. Importantly, dronabinol was capable to release the differentiation blockage of both clones – leading to granulocytic (clone 1) as well as monocytoid differentiation (clone 2). This observation strongly suggests that dronabinol has targeted the leukemia initiating clone.

Cytogenetic assessment of a sample obtained at diagnosis, which revealed a normal karyotype in 44 cells, but a partial deletion of the long arm of chromosome 7 [del(7)(q32)] in 10 mitoses (mos46,XY,del(7)(q32) [10]/46,XY [44], supplemental Fig. S5) supports this notion:

This del(7q)-cohort precedes a monosomal clone with complete loss of chromosome 7. MLPA at diagnosis and in a follow up sample is provided with Fig. 8b – demonstrating disease plasticity and leukemia evolution.

Importantly, acquisition of monosomy 7 did not influence release of the differentiation blockage of leukemia blasts upon exposure to dronabinol, further indicating that dronabinol targets the initiating leukemic clone [33].

3.10. Dronabinol-driven antileukemic activity depends on OGT

We next addressed, whether antileukemic efficacy in response to dronabinol seen in this patient depends on OGT as well:

First, OGT expression at diagnosis and two months into the treatment with dronabinol was assessed flow cytometrically: Upregulation of OGT expression was observed in the patient sample taken two months after start of treatment (Fig. 9a).

To validate, this effect was mimicked ex vivo: a sample of this patient taken at diagnosis was treated with dronabinol for 48 h – and statistically relevant upregulation of OGT was confirmed by flow cytometry (Fig. 9b).

Furthermore, to determine ex vivo cytoreductive sensitivity towards dronabinol in dependence to OGT, a sample taken at diagnosis was cultured ex vivo, OGT-interferenced, and treated with dronabinol in serial dilutions for 48 h. Indeed, potent OGT-dependent cytoreduction of the viable cell clone was noted (Fig. 9c).

3.11. In vitro modeling of OGT-dependent release of the differentiation blockage of acute myeloid leukemia cells upon exposure to dronabinol

Capacity of release of the differentiation blockage in response to dronabinol was confirmed in an independent well characterized
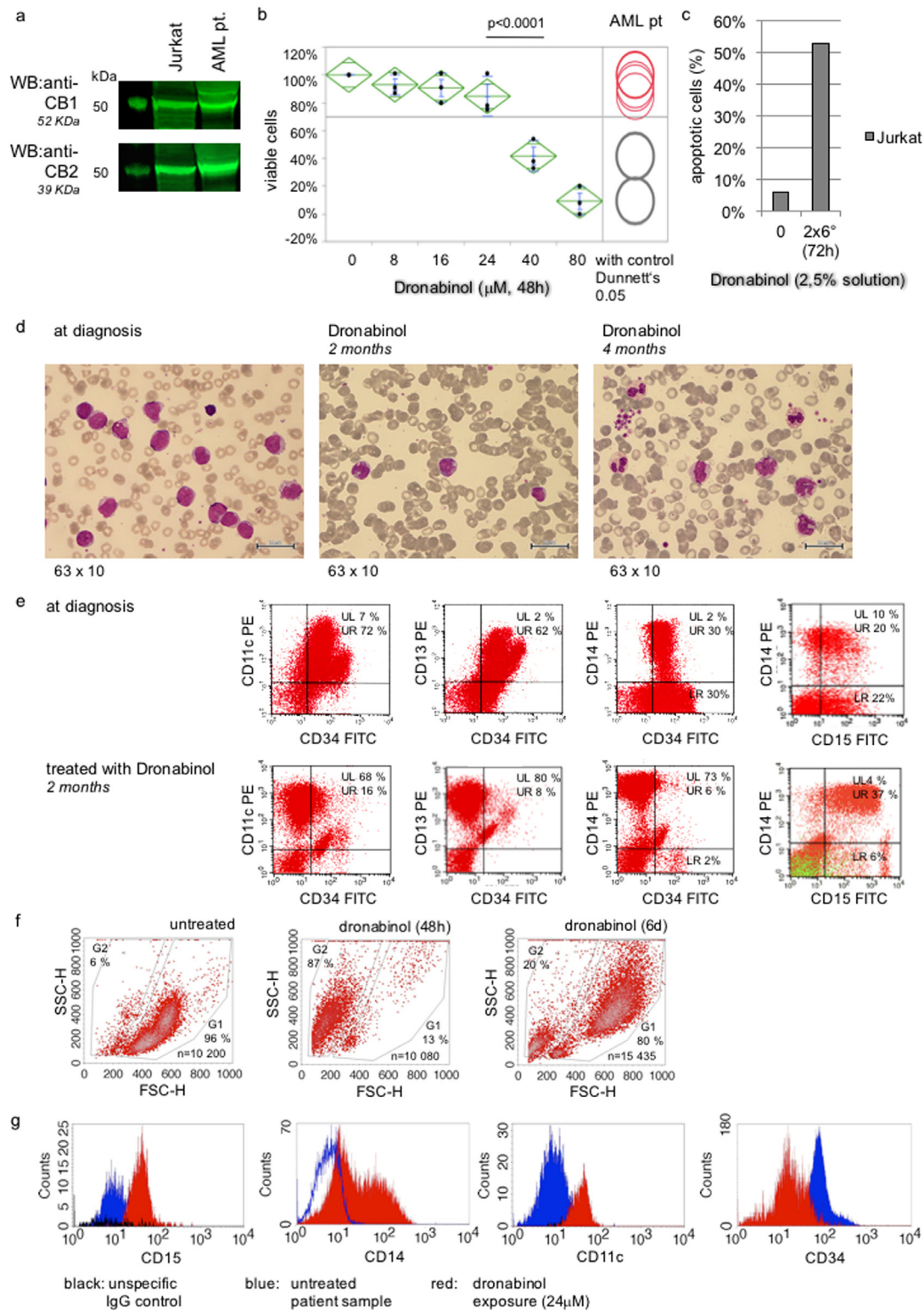
Fig. 7. **Dronabinol targets the leukemia clone in a patient with AML *in vivo* and *ex vivo*.** (a) Representative western immunoblot expression of the cannabinoid receptors CB1/2. Jurkat cells serve as positive controls. First lane: protein ladder. (b) FSC/SSC-based flow cytometry assay to determine the viable population after treatment with dronabinol *ex vivo*. Statistical significance at $p < 0.05$ (one-way ANOVA), with control (Dunnett'ps). Drug-carrier control assays, which did not reveal any significant antileukemic effects at the highest concentration used up to 80 microM, were provided earlier (Kampa-Schittenhelm et al., 2016). (c) Representative plasma-inhibitory assay (PIA) using donor serum (w/o dronabinol) or patient serum while on treatment with dronabinol 2,5% 6 drops BID to culture Jurkat cells. Proapoptotic efficacy is determined using an Annexin V/ropidium iodide-based flow cytometry assay. (d) Course of disease, cytomorphology: May-Gruenwald-Giemsa stain of patient samples at diagnosis (left panel) and treatment with dronabinol for 2 (mid panel) and 4 months (right panel). (e) Course of disease, immunophenotype: Patient sample at diagnosis (upper panels) and two months into treatment with dronabinol (lower panels); right panel: CD5 overlay (green) excludes coexpression. (f/g) Differentiation of native leukemic blasts upon treatment with dronabinol: Representative analyses of *ex vivo* culture of patient sample treated with dronabinol assessed by flow cytometry. (f) FSC/SSC density plots. (g) Representative graphs of relative expression of CD11c, CD15 (incubation time 48 h), CD14 and CD34 (incubation time 6 days) in response to dronabinol assessed by flow cytometry.
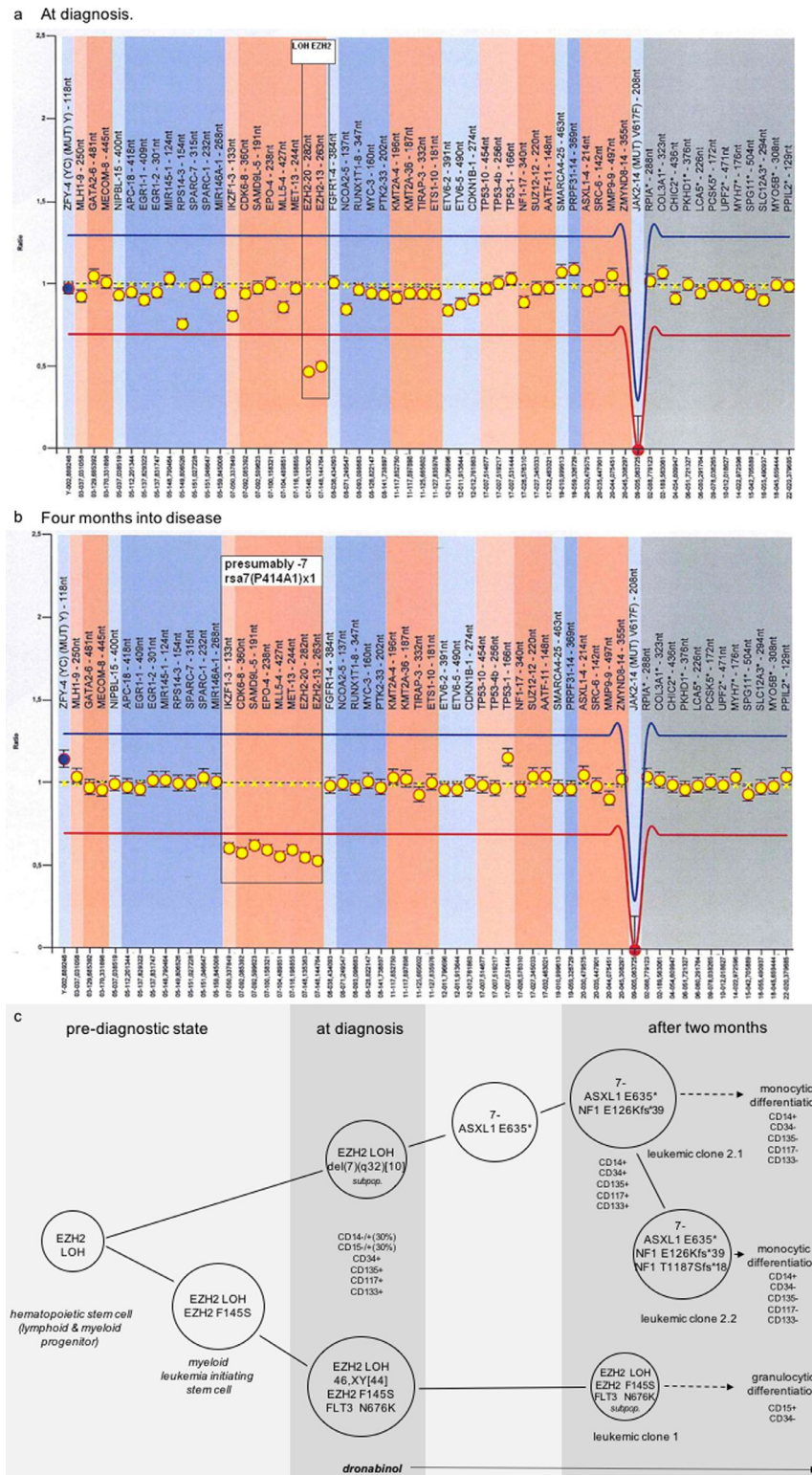
Fig. 8. MLPA reveals molecular leukemic evolution over time. (a) Deletion/duplication analysis reveals deletion of EZH2 (LOH) at diagnosis. LOH (loss of heterocygosity). (b) Deletion/duplication analysis by MLPA shows region specific deletions in 7q as well as 7p compatible with monosomy 7 at 4 months into disease. rsa7(P414-A1) x 1 (region specific assay). (c) Depiction of mutation analysis of reported patient treated with dronabinol demonstrates clonal evolution into leukemic subclones and differentiation into mature granulocytes and monocytes. Immunophenotypes assessed by flow cytometry are comparatively provided.

leukemia model: MOLM14 cells, harboring a FLT3 ITD gain-of-function mutation, have been previously shown to block myeloid differentiation via suppression of CCAAT/enhancer-binding protein alpha (C/EBPalpha) expression [34].

Thus, cells were treated with dronabinol in a sub-IC50 concentration (20 μM) for 48 h and changes in C/EBPalpha protein expression were monitored over time by Western immunoblot – and confirmed independently on the mRNA level. C/EBPalpha is thereby upregulated upon
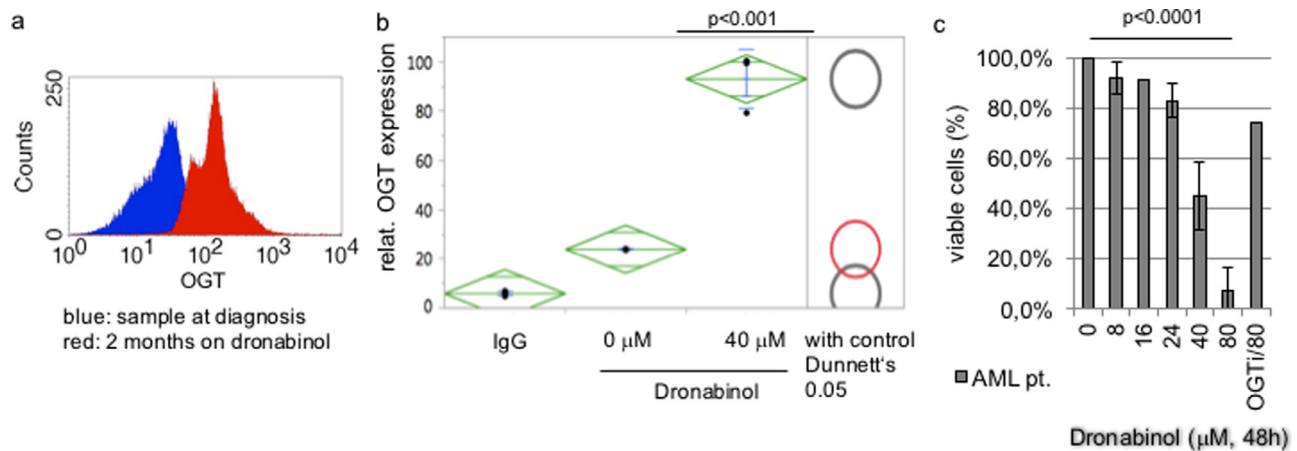
Fig. 9. OGT dependent release of the differentiation blockage upon treatment with dronabinol in AML leukemia cells. (a) Representative analysis of *in vivo* OGT expression in a patient prior to and two months after start of treatment with dronabinol. (b) OGT expression, as assessed by flow cytometry, in a patient sample taken at diagnosis and treated with dronabinol *ex vivo*. (c) FSC/SSC-based flow cytometry assay to determine the viable population after treatment of pt's native leukemic blasts with dronabinol for 48 h *ex vivo*. OGT-interference demonstrates effective rescue of the patient sample treated with the highest tested dose at 80 μM. Statistical significance at $p < 0.05$ (one-way ANOVA), $n = 3$.

treatment with dronabinol in a time-dependent manner (Fig. 10a/b) — leading to consecutive CD11c expression (Fig. 10c). This observation is of special interest, as it has been previously shown that C/EBPalpha directly links to the mediation of CD11c expression [35].

This observation independently validates our observation that dronabinol is capable of overriding the differentiation blockage in acute leukemia cells.

In analogy to the findings in the Jurkat model (compare Fig. 5d), we used the OGA-selective inhibitor TMG in our MOLM14 model to cross-validate whether cellular differentiation is truly mediated via O-GlcNAcylation. Similar to dronabinol, exposure of blasts towards TMG resulted in an increase of *C/EBPalpha* levels (supplemental Fig. S6a).

We also used this model to demonstrate OGT-dependency: Western immunoblotting confirmed upregulation of OGT protein expression levels in response to dronabinol in a time-dependent manner (Fig. 10d), which is validated on the mRNA level (Fig. 10e).

Next, stably lentivirally suppressed OGTi MOLM14 cell strains were established, treated with dronabinol and probed for CD11c expression versus a negative control or the parental cell strains. Fig. 10f demonstrates successful transduction of OGT shRNA plasmid or an empty vector negative control in the MOLM14 cell line. Stable suppression of OGT protein expression is shown in Fig. 10g.

Using a standard flow cytometry protocol, exposure of cells towards dronabinol for 72 h revealed upregulation of CD11c — whereas, stable suppression of OGT abrogated increase of CD11c in the OGTi cell strains (Fig. 10h).

To summarize, our findings provide strong evidence that dronabinol exerted antileukemic efficacy via OGT-linked mechanisms in acute lymphoid and myeloid leukemia *in vivo, ex vivo* and in *in vitro* models.

4. Discussion

In recent years, the O-linked β-N-acetyl glucosamine (O-GlcNAc) transferase (*OGT*) gained increasing attention as a major cellular signaling mechanism adding O-GlcNAc to serine or threonine residues, which rivals with other post-translational modifications such as phosphorylation. In fact, many proteins are capable of being post-translationally modified by both, O-GlcNAc and phosphate (reviewed by Hart and colleagues [36]). Aberrant O-GlcNAc modification is implicated in pathologies of metabolic and neurodegenerative diseases as well as cancers and autoimmunity (reviewed by Bond and Hanover [9]). In cancer-relevant processes, O-GlcNAcylation is involved in cell signaling, transcription, cell division, metabolism and cytoskeletal regulation (summarized by Slawson and Hart [37]).

Interestingly in early hematopoiesis, recent data suggest a role of O-GlcNAc homeostasis to disrupt transcriptional programs to control cell fate decisions [38]. However, little is known about specific mechanisms in malignant hematology, especially in acute leukemia — and it becomes increasingly clear that mechanisms are complex, in part contradictory and depend on the molecular background of the models studied.

We provide evidence that dronabinol is a potent epigenetic modifier of gDNA methylation patterns, potentially affecting changes of expression of several genes. *OGT* was identified as the highest altered gene via hypomethylation of the transcription start site (TSS). This effect translates into increased mRNA and protein expression levels with consecutive propelled O-GlcNAcylation.

In our models, OGT seemed to play a central role in the antileukemic efficacy observed for dronabinol. Interestingly, two different mechanisms become apparent:

While higher concentrations of dronabinol lead to induction of apoptosis, a second phenomenon can be observed for sub-lethal dosing, where dronabinol mediates release of the differentiation blockage of leukemia blasts *in vitro, ex vivo* as well as *in vivo* in an OGT-dependent manner.

Our observation is supported by independent reports stating a role of OGT in apoptosis as well as cellular differentiation: Shi and colleagues have demonstrated that O-GlcNAcylation promotes induction of apoptosis via dephosphorylation and competitive O-GlcNAc modification of threonine and serine residues at AKT and BAD [39].

Secondly, several independent reports implicate a role of O-GlcNAcylation in lymphoid (T-cell) as well as myeloid cellular maturation: Inoue and colleagues have shown that myeloid differentiation is mediated via stabilization of ASXL1 by O-GlcNAcylation [13]. Another report describes an OGT-EZH2 regulatory axis, which is abrogated by mutation/LOH [40]. This is of interest as both (pre)leukemic epigenetic modifiers are known to drive leukemia-originating stem cell clones [33].

Intriguingly, for the presented AML case report repetitive molecular analysis at diagnosis and during follow up allowed to denominate the putative initiating pre-leukemic lesion as a loss of one copy of *EZH2* (LOH), which was present at diagnosis and may have fueled acquisition of additional mutations. In this context, an ASXL1 mutation was detected in a developing subclone.

While the exact mechanisms will need to be elucidated in detail, it is highly suggestive that dronabinol-mediated increase of OGT levels results in a direct interaction with O-GlcNAcylation and stabilization of these target proteins. This hypothesis is further backed by a recent report describing opposite functions of EZH2 at early and late stages
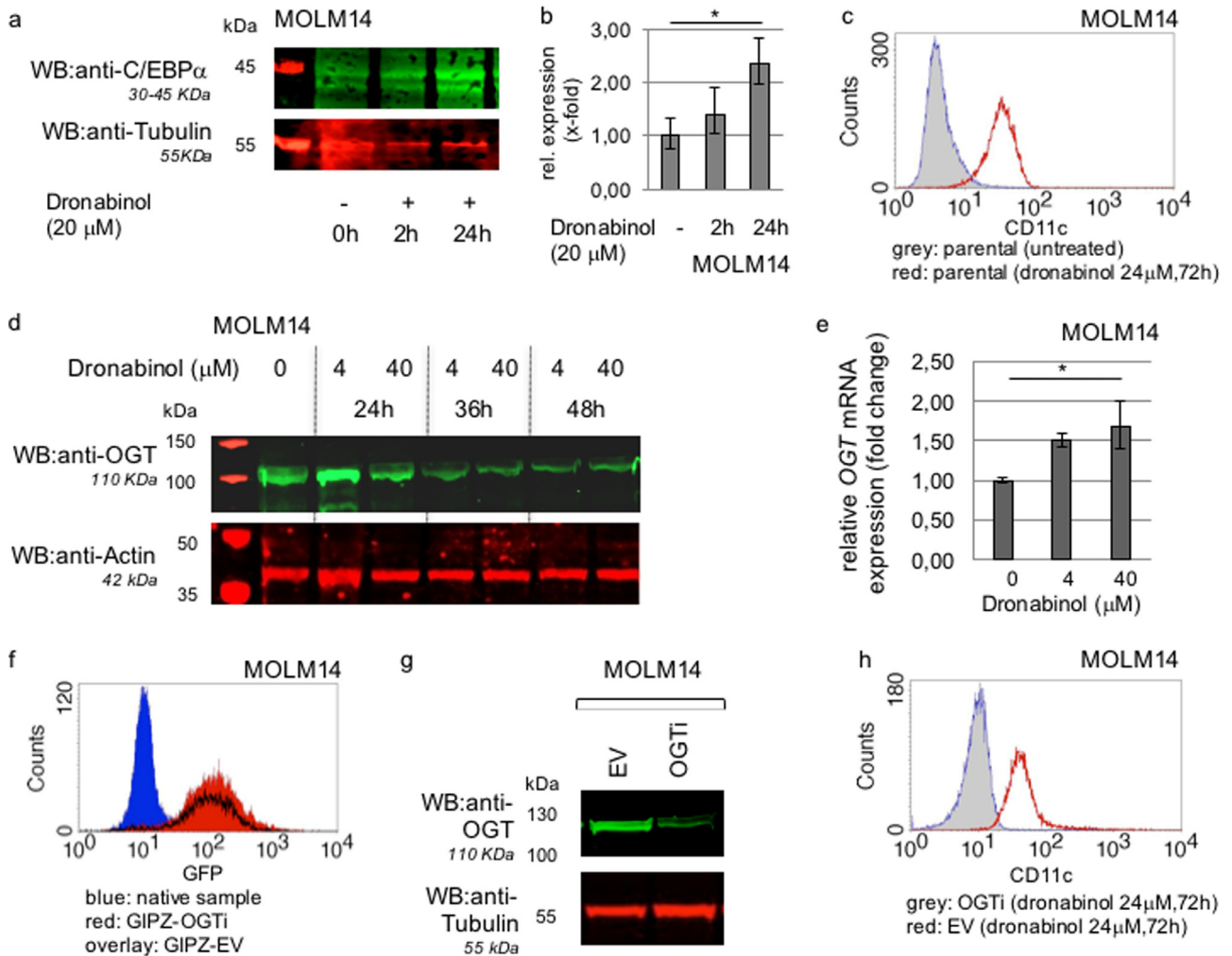
Fig. 10. In vitro modeling of release of the differentiation blockage upon treatment with dronabinol. (a) Representative western immunoblot for C/EBPalpha expression in response to dronabinol in MOLM14 leukemia cells. Probing for Tubulin serves as a loading control. First lane: protein ladder. (b) qRT-PCR approach to measure *C/EBPalpha* mRNA expression levels in response to dronabinol. * significance at $p < 0.05$ (t-test). (c) Representative flow cytometry assay to determine relative expression of CD11c in MOLM14 cells as assessed by flow cytometry in response to dronabinol. (d) Representative western immunoblot for OGT expression in response to dronabinol. Probing for Actin serves as loading control. First lane: protein ladder. (e) qRT-PCR of MOLM14 cells treated with dronabinol for 24 h. Relative fold change of OGT expression levels are shown. * confidence interval 95%. GAPDH serves as housekeeping gene. (f) OGT-interference in MOLM14 cells: Flow cytometry assay to determine transduction efficiency as assessed by green fluorescence protein (GFP) reactivity. GIPZ-OGTi (lentiviral plasmid OGT shRNA vector), EV (empty vector control). (g) Representative western immunoblot demonstrating successful suppression of OGT translation. EV (empty vector control). Probing for tubulin serves as loading control. (h) Representative analyses of relative expression of CD11c as assessed by flow cytometry in response to dronabinol. OGT-interferenced (OGTi) MOLM14 cells vs. empty vector control cell strains.

of disease: While EZH2 acts as a tumor suppressor at induction of oncogenesis, oncogenic properties are found to maintain the disease [41]. This observation also explains the use und usefulness of EZH2 inhibitors to suppress disease maintenance – while reconstitution of EZH2 functionality at early stages, as suggested by our findings via targeting the OGT-EZH2 regulatory axis, may target the actual leukemia initiating clone.

To make it even more complex, a recent report states that suppression of O-GlcNAc activity leads to differentiation of leukemic blasts [42]. At first sight, this observation challenges the data presented herein – and even though we might not be able to fully explain all the discrepancies, several obvious issues need to be accounted for. Besides technical differences with regard to culture conditions and assessment of differentiation, some cell models such as HL60 used in the competing report, are well known to spontaneously differentiate [43], which may account for false-positive results, including the knock-out models.

But most importantly, we have used molecularly differing leukemia models, which most likely respond differently to modulators such as dronabinol described herein as an epigenetically active drug.

Dronabinol affects the methylation status of hundreds of genes – including OGT, which again globally orchestrates hundreds of proteins via O-GlcNAcylation. Even more, O-GlcNAcylation may compete with phosphorylation of serine or threonine residues, which again depends on various factors including distinct gene mutation profiles differing in between leukemia subentities.

Thus again, context specificity, as reported and discussed above for EZH2 mutations, likely plays a major role in the complex mechanisms of cellular differentiation of leukemic blasts.

Consequently, pre-definition of distinct molecular subentities will be essential for future studies and clinical trials.

In addition to the patient with AML described above, and further strengthening our observations, we demonstrate clinical activity of dronabinol in another patient, suffering from relapsing T-lymphoblastic lymphoma/leukemia: Molecular fingerprinting of a CDKN2A mutation, detected in an NGS mutation screen, traced back a maturing population to the leukemia blast population. In this context, it is utmost remarkable that a recent report has demonstrated glucose metabolism and O-GlcNAcylation to be essential for T-cell maturation and activation [44]. One might speculate that it is the combination of

dexamethasone pretreatment (increasing glucose levels) plus dronabinol (increasing OGT levels), which may have lead to the observed cellular maturation effect in this patient – and this approach should further be followed in future studies.

While we have stringent evidence that dronabinol has clinical activity with regard to overriding the differentiation blockage in leukemia cells – dronabinol may have exhibited additional cytoreductive potency in both reported patients as well. However this effect, as demonstrated in *ex vivo* assays and corresponding Jurkat (T-ALL) and MOLM14 (mutat-FLT3) leukemia cell line models, was obscured *in vivo* due to initial cytoreductive co-medication with hydroxyurea, respectively dexamethasone. Still, the cytoreductive property of dronabinol is backed by several previous reports, describing potent *in vitro* and *ex vivo* cytoreduction of lymphoblastic and leukemia cell lines, including Jurkat and MOLM14 cells, as well as native leukemia cells [17,45]. In addition, a recent case report described potent *in vivo* cytoreduction in a patient with Ph+ALL treated with cannabis extracts [46].

Tantalizingly, we provide preliminary data linking hypomethylation of a distinct locus within the TSS of *OGT* to a putative tumor suppressor gene, which possesses far-reaching consequences for future directions of research:

A database search maps this significantly altered methylation probe within the TSS of *OGT* to the binding site of the *LIN-9 DREAM MuvB Core Complex Component (LIN9)* transcription factor (LIN9 binding site at chrX 70668596−70669446) [47,48], a suggested haploinsufficient tumor suppressor and regulator of embryonic development [49]. Furthermore, LIN9 is linked to the control of proliferation and cell cycle checkpoints in embryonic stem cells [50]. However, virtually nothing is known about a potential role of *LIN9* in leukemogenesis or G-protein coupled/cannabinoid receptor signaling.

Interestingly, we have preliminary evidence that LIN9 indeed modulates CD45 expression levels in acute leukemia cells as demonstrated in *LIN9* knock-out/knock-in Jurkat cell models (supplemental Fig. S7a−c). Systematic elaboration of expression and function of LIN9 in leukemia is warranted – and subject of ongoing systematic studies.

Noteworthy, a second probe within the TSS was identified in the 27K array and confirmed in the 450 K array, which did not display any significant alterations in methylation patterns upon exposure to dronabinol (compare supplemental Tables S2 and S3).

Excitingly, this second (unaffected) probe detected in both methylation arrays, links to the binding site of the retinoic acid receptor alpha (RARα, binding site at chrx 70668524−70669748) [51]. RARα is extensively studied in leukemia research due to the high clinical efficacy in acute promyelocytic leukemia (reviewed by de Thé and Chen [52]). The antileukemic effect mediated via activation of RARα is thereby mainly based on overriding the differentiation blockage in acute leukemia blasts. Intriguingly, this effect has been previously linked, at least in part, to direct interaction of RARα with OGT (however, this observation needs reconfirmation [12]).

It is tempting to speculate, that dronabinol exerts similar effects on maturation of leukemic blasts via epigenetic activation of an alternative transcription factor binding site, allowing initiation of *OGT* transcription via LIN9 instead of RARα.

The consequences are far reaching, providing an approach to override the differentiation blockage in non-promyelocytic leukemia as described herein in two patients.

Clinical use of cannabinoids such as dronabinol may also provide an alternative strategy to target (e.g. retinoic acid-resistant) promyelocytic leukemia. In this context, we provide preliminary data in a patient with newly diagnosed APL, showing that indeed both ATRA but also dronabinol are capable to induce differentiation of the leukemic blasts *ex vivo* (supplemental Fig. S7d).

In fact, dronabinol possesses well established clinical activities, which lead to FDA-approval in the United States as Marinol® for the treatment of chemotherapy-induced nausea and vomiting or stimulation of appetite associated with weight loss in patients with AIDS.

Furthermore, antitumor efficacy of THC is increasingly recognized: Several reports have suggested growth-inhibition in a number of hematologic and solid tumor cancer models, including animal models and early phase II trials, arguing for the beneficial use of cannabinoids as low-toxic anticancer therapeutics (Short and Little on behalf of the *Cannabinoid in Recurrent Glioma Study Group* [53] and review by Guzman [54]). In this context, THC together with non-psychoactive cannabidiol (CBD) has gained orphan drug status by the FDA (CBD) and EMA (THC:CBD) as an anticancer treatment of glioma.

In line, and further supported by a recent case report [46], we have demonstrated that THC exerts direct proapoptotic efficacy in a subset of native acute leukemia blasts treated *ex vivo* [17].

Dronabinol has an excellent safety profile. Due to sparse densities of cannabinoid receptors in lower brainstem areas, which control cardiovascular and respiratory functions [55], LC50s are not defined and dose-limiting side effects, if any, may be due to modest cardiovascular effects by lowering blood pressure and heart rate [56].

However, based on the findings reported herein, the use of dronabinol as antitumor treatment may as well possess the potential to induce severe complications such as differentiation syndrome (also known as retinoic acid syndrome as best characterized for ATRA-treated patients with APL), which is a life threatening condition, leading to massive cellular migration of differentiating leukemic cells, endothelial activation, and release of interleukins and vascular factors responsible for tissue damage. Clinically, this results in symptoms such as unexplained fever, acute respiratory distress with interstitial pulmonary infiltrates, and/or a vascular capillary leak syndrome leading to acute renal failure (summarized by Montesinos and colleagues in [57]).

Referring to the ongoing public interest and discussions about legal issues of cannabinoids – in our opinion, the medicinal use of cannabinoids as anticancer therapy should remain restricted to the hands of experienced oncologists.

To summarize, our findings provide several aspects of interest for future cancer research and therapeutic strategies: (A) We provide a strong rationale for exploring dronabinol as an agent with remarkable antileukemic efficacy achievable *in vivo*. (B) The data sheds light on a two-step mechanism with induction of apoptosis in higher doses – and, excitingly, overriding the differentiation blockage in sublethal concentrations. Intriguingly, dronabinol thereby targets the originating leukemia clone. (C) Dronabinol acts as an unselective epigenetic modifier, potently affecting expression levels of a multitude of genes. Among the top altered genes, we have identified OGT as a major regulator of apoptosis and differentiation in leukemia cells, which provides the rationale for further investigation of O-GlcNAcylation in acute leukemia and tumorigenesis in general. O-GlcNAcylation of serine and threonine residues may thereby function as a competitive mechanism to phosphorylation and act as an important (therapeutically targetable) mechanism in tumor cell signaling. Whether other proteins, targeted by O-GlcNAcylation, or additional genes, affected by changes of methylation patterns as a response to dronabinol, contribute to the observed cellular effects is not known. Further, to date, functional roles of many of the highest altered genes in our methylation arrays are not well characterized. These topics need to be addressed in detail in defined cellular backgrounds and in specific subentities (e.g. *EZH2* mutated myeloid neoplasms) in future studies.

To conclude, our data provide proof-of-principle for further systematic evaluation of the distinct antileukemic efficacy of cannabinoids in leukemia subentities – and clinical evaluation is warranted.

Author's contribution

K.KS designed the research study, performed the functional models, analyzed the data and wrote the paper. T.H. and I.B. performed

the molecular modeling and contributed with data analysis and writing of the paper. M.B. performed the microarray assays and contributed with data analysis and writing of the paper. HJ.B. performed the cell sorting experiments. G.B. performed statistical analyses, V.T., F.A., L.A.H., S.T.D. and B.I. performed the functional models. T.G. performed proteomic analyses, U.MH. performed the cytogenetic model and contributed with data analysis and writing of the paper. E.S. contributed to research design of the O-GlcNAcylation models, analysis of data and writing of the paper. W.V. performed the cytomorphology experiments and contributed with data analysis and writing of the paper. M.S. designed the research study, analyzed clinical and experimental data and wrote the paper.

Declaration of Competing Interest

The authors declare no competing financial interests.

Acknowledgements

Funding

Supplementary materials

Supplementary material associated with this article can be found, in the online version, at doi:10.1016/j.ebiom.2020.102678.

References

[1] Network TCGAR. Genomic and epigenomic landscapes of adult de novo acute myeloid leukemia. N Engl J Med 2013;368(22):2059–74.
[2] Ding L, Ley TJ, Larson DE, Miller CA, Koboldt DC, Welch JS, et al. Clonal evolution in relapsed acute myeloid leukaemia revealed by whole-genome sequencing. Nature 2012;481(7382):506–10.
[3] Welch JS, Ley TJ, Link DC, Miller CA, Larson DE, Koboldt DC, et al. The origin and evolution of mutations in acute myeloid leukemia. Cell 2012;150(2):264–78.
[4] Lo-Coco F, Avvisati G, Vignetti M, Thiede C, Orlando SM, Iacobelli S, et al. Retinoic acid and arsenic trioxide for acute promyelocytic leukemia. N Engl J Med 2013;369(2):111–21.
[5] DiNardo CD, Stein EM, de Botton S, Roboz GJ, Altman JK, Mims AS, et al. Durable remissions with ivosidenib in IDH1-mutated relapsed or refractory AML. N Engl J Med 2018;378(25):2386–98.
[6] Stein EM, DiNardo CD, Pollyea DA, Fathi AT, Roboz GJ, Altman JK, et al. Enasidenib in mutant IDH2 relapsed or refractory acute myeloid leukemia. Blood 2017;130 (6):722–31.
[7] Kampa-Schittenhelm KM, Vogel W, Bonzheim I, Fend F, Horger M, Kanz L, et al. Dasatinib overrides the differentiation blockage in a patient with mutant-KIT D816V positive CBFbeta-MYH11 leukemia. Oncotarget 2018;9(14):11876–82.

[8] Sexauer A, Perl A, Yang X, Borowitz M, Gocke C, Rajkhowa T, et al. Terminal myeloid differentiation in vivo is induced by FLT3 inhibition in FLT3/ITD AML. Blood 2012;120(20):4205–14.
[9] Bond MR, Hanover JA. A little sugar goes a long way: the cell biology of O-GlcNAc. J Cell Biol 2015;208(7):869–80.
[10] Yang X, Qian K. Protein O-GlcNAcylation: emerging mechanisms and functions. Nat Rev Mol Cell Biol 2017;18(7):452–65.
[11] Chikanishi T, Fujiki R, Hashiba W, Sekine H, Yokoyama A, Kato S. Glucose-induced expression of MIP-1 genes requires O-GlcNAc transferase in monocytes. Biochem Biophys Res Commun 2010;394(4):865–70.
[12] Fujiki R, Chikanishi T, Hashiba W, Ito H, Takada I, Roeder RG, et al. GlcNAcylation of a histone methyltransferase in retinoic-acid-induced granulopoiesis. Nature 2009;459(7245):455–9.
[13] Inoue D, Fujino T, Sheridan P, Zhang YZ, Nagase R, Horikawa S, et al. A novel ASXL1-OGT axis plays roles in H3K4 methylation and tumor suppression in myeloid malignancies. Leukemia 2018;32(6):1327–37.
[14] Kang ES, Han D, Park J, Kwak TK, Oh MA, Lee SA, et al. O-GlcNAc modulation at Akt1 Ser473 correlates with apoptosis of murine pancreatic beta cells. Exp Cell Res 2008;314(11−12):2238–48.
[15] Bauer C, Gobel K, Nagaraj N, Colantuoni C, Wang M, Muller U, et al. Phosphorylation of TET proteins is regulated via O-GlcNAcylation by the O-linked N-acetylglucosamine transferase (OGT). J Biol Chem 2015;290(8):4801–12.
[16] Dey A, Seshasayee D, Noubade R, French DM, Liu J, Chaurushiya MS, et al. Loss of the tumor suppressor BAP1 causes myeloid transformation. Science 2012;337 (6101):1541–6.
[17] Kampa-Schittenhelm KM, Salitzky O, Akmut F, Illing B, Kanz L, Salih HR, et al. Dronabinol has preferential antileukemic activity in acute lymphoblastic and myeloid leukemia with lymphoid differentiation patterns. BMC Cancer 2016;16(1):25.
[18] Kampa-Schittenhelm KM, Heinrich MC, Akmut F, Dohner H, Dohner K, Schittenhelm MM. Quizartinib (AC220) is a potent second generation class III tyrosine kinase inhibitor that displays a distinct inhibition profile against mutant-FLT3, -PDGFRA and -KIT isoforms. Mol Cancer 2013;12:19.
[19] Cox J, Mann M. MaxQuant enables high peptide identification rates, individualized p.p.b.-range mass accuracies and proteome-wide protein quantification. Nat Biotechnol. 2008;26(12):1367–72.
[20] Levis M, Brown P, Smith BD, Stine A, Pham R, Stone R, et al. Plasma inhibitory activity (PIA): a pharmacodynamic assay reveals insights into the basis for cytotoxic response to FLT3 inhibitors. Blood 2006;108(10):3477–83.
[21] Brenet F, Moh M, Funk P, Feierstein E, Viale AJ, Socci ND, et al. DNA methylation of the first exon is tightly linked to transcriptional silencing. PLoS One 2011;6(1): e14524.
[22] Hermiston ML, Xu Z, Weiss A. CD45: a critical regulator of signaling thresholds in immune cells. Annu Rev Immunol. 2003;21:107–37.
[23] Pulido R, Sanchez-Madrid F. Glycosylation of CD45: carbohydrate composition and its role in acquisition of CD45R0 and CD45RB T cell maturation-related antigen specificities during biosynthesis. Eur J Immunol. 1990;20(12):2667–71.
[24] Bene MC, Nebe T, Bettelheim P, Buldini B, Bumbea H, Kern W, et al. Immunophenotyping of acute leukemia and lymphoproliferative disorders: a consensus proposal of the European LeukemiaNet Work Package 10. Leukemia 2011;25 (4):567–74.
[25] Ratei R, Karawajew L, Lacombe F, Jagoda K, Del Poeta G, Kraan J, et al. Normal lymphocytes from leukemic samples as an internal quality control for fluorescence intensity in immunophenotyping of acute leukemias. Cytometry B Clin Cytom. 2006;70(1):1–9.
[26] Stewart M, Thiel M, Hogg N. Leukocyte integrins. Curr Opin Cell Biol. 1995;7 (5):690–6.
[27] Bullard DC, Hu X, Adams JE, Schoeb TR, Barnum SR. p150/95 (CD11c/CD18) expression is required for the development of experimental autoimmune encephalomyelitis. Am J Pathol. 2007;170(6):2001–8.
[28] Huleatt JW, Lefrancois L. Antigen-driven induction of CD11c on intestinal intraepithelial lymphocytes and CD8+ T cells in vivo. J Immunol. 1995;154(11):5684–93.
[29] Yuzwa SA, Macauley MS, Heinonen JE, Shan X, Dennis RJ, He Y, et al. A potent mechanism-inspired O-GlcNAcase inhibitor that blocks phosphorylation of tau in vivo. Nat Chem Biol. 2008;4(8):483–90.
[30] Arber DA, Orazi A, Hasserjian R, Thiele J, Borowitz MJ, Le Beau MM, et al. The 2016 revision to the World Health Organization classification of myeloid neoplasms and acute leukemia. Blood 2016;127(20):2391–405.
[31] Boudry-Labis E, Roche-Lestienne C, Nibourel O, Boissel N, Terre C, Perot C, et al. Neurofibromatosis-1 gene deletions and mutations in de novo adult acute myeloid leukemia. Am J Hematol. 2013;88(4):306–11.
[32] Heidel F, Solem FK, Breitenbuecher F, Lipka DB, Kasper S, Thiede MH, et al. Clinical resistance to the kinase inhibitor PKC412 in acute myeloid leukemia by mutation of Asn-676 in the FLT3 tyrosine kinase domain. Blood 2006;107(1):293–300.
[33] Hou HA, Tien HF. Mutations in epigenetic modifiers in acute myeloid leukemia and their clinical utility. Expert Rev Hematol. 2016;9(5):447–69.
[34] Zheng R, Friedman AD, Levis M, Li L, Weir EG, Small D. Internal tandem duplication mutation of FLT3 blocks myeloid differentiation through suppression of C/ EBPalpha expression. Blood 2004;103(6):1883–90.
[35] Drescher B, Nagel S, Krauter J, Heidenreich O, Ganser A, Heil G. AML1/ETO inhibits AML1/CCAAT-enhancer binding protein-alpha mediated activation of the CD11c promoter and represses CD11c expression in HL60 cells. Haematologica 2003;88 (8):956–8.
[36] Hart GW, Slawson C, Ramirez-Correa G, Lagerlof O. Cross talk between O-GlcNAcylation and phosphorylation: roles in signaling, transcription, and chronic disease. Annu Rev Biochem. 2011;80:825–58.

[37] Slawson C., Hart G.W.O-GlcNAc signalling: implications for cancer cell biology. Nat Rev Cancer.11(9):678-84.

[38] Zhang Z, Parker MP, Graw S, Novikova LV, Fedosyuk H, Fontes JD, et al. O-GlcNAc homeostasis contributes to cell fate decisions during hematopoiesis. J Biol Chem 2019;294(4):1363–79.

[39] Shi J, Gu JH, Dai CL, Gu J, Jin X, Sun J, et al. O-GlcNAcylation regulates ischemia-induced neuronal apoptosis through AKT signaling. Sci Rep 2015;5:14500.

[40] Chu CS, Lo PW, Yeh YH, Hsu PH, Peng SH, Teng YC, et al. O-GlcNAcylation regulates EZH2 protein stability and function. Proc Natl Acad Sci U S A 2014;111(4):1355–60.

[41] Basheer F, Giotopoulos G, Meduri E, Yun H, Mazan M, Sasca D, et al. Contrasting requirements during disease evolution identify EZH2 as a therapeutic target in AML. J Exp Med 2019;216(4):966–81.

[42] Asthana A, Ramakrishnan P, Vicioso Y, Zhang K, Parameswaran R. Hexosamine Biosynthetic Pathway Inhibition Leads to AML Cell Differentiation and Cell Death. Mol Cancer Ther. 2018;17(10):2226–37.

[43] Palis J, King B, Keng P. Separation of spontaneously differentiating and cell cycle-specific populations of HL-60 cells. Leuk Res. 1988;12(4):339–44.

[44] Swamy M., Pathak S., Grzes K.M., Damerow S., Sinclair L.V., van Aalten D.M., et al. Glucose and glutamine fuel protein O-GlcNAcylation to control T cell self-renewal and malignancy. Nat Immunol.17(6):712-20.

[45] McKallip RJ, Lombard C, Fisher M, Martin BR, Ryu S, Grant S, et al. Targeting CB2 cannabinoid receptors as a novel therapy to treat malignant lymphoblastic disease. Blood 2002;100(2):627–34.

[46] Singh Y, Bali C. Cannabis extract treatment for terminal acute lymphoblastic leukemia with a Philadelphia chromosome mutation. Case Rep Oncol 2013;6(3):585–92.

[47] Xu LM, Li JR, Huang Y, Zhao M, Tang X, Wei L. AutismKB: an evidence-based knowledgebase of autism genetics. Nucleic Acids Res 2012;40(Database issue): D1016–22.

[48] Litovchick L, Sadasivam S, Florens L, Zhu X, Swanson SK, Velmurugan S, et al. Evo-lutionarily conserved multisubunit RBL2/p130 and E2F4 protein complex represses human cell cycle-dependent genes in quiescence. Mol Cell 2007;26 (4):539–51.

[49] Reichert N, Wurster S, Ulrich T, Schmitt K, Hauser S, Probst L, et al. Lin9, a subunit of the mammalian DREAM complex, is essential for embryonic development, for survival of adult mice, and for tumor suppression. Mol Cell Biol. 2010;30 (12):2896–908.

[50] Esterlechner J, Reichert N, Iltzsche F, Krause M, Finkernagel F, Gaubatz S. LIN9, a subunit of the DREAM complex, regulates mitotic gene expression and proliferation of embryonic stem cells. PLoS One 2013;8(5):e62882.

[51] Hua S, Kittler R, White KP. Genomic antagonism between retinoic acid and estrogen signaling in breast cancer. Cell 2009;137(7):1259–71.

[52] de The H, Chen Z. Acute promyelocytic leukaemia: novel insights into the mechanisms of cure. Nat Rev Cancer 2010;10(11):775–83.

[53] Group TCiRGS, SC Short, Little C. ACTR-56. A¬†2-part safety and exploratory efficacy randomised double-blind, placebo-controlled study of A¬†1:1 ratio of cannabidiol and delta-9-tetrahydrocannabinol (CBD:THC) plus dose-intense temozolomide in patients with recurrent glioblastoma multiforme (GBM). Neuro-Oncology 2017;19(suppl_6) vi13-vi.

[54] Guzman M. Cannabinoids: potential anticancer agents. Nat Rev Cancer 2003;3 (10):745–55.

[55] Herkenham M, Lynn AB, Little MD, Johnson MR, Melvin LS, de Costa BR, et al. Cannabinoid receptor localization in brain. Proc Natl Acad Sci U S A 1990;87 (5):1932–6.

[56] Gorelick DA, Goodwin RS, Schwilke E, Schwope DM, Darwin WD, Kelly DL, et al. Tolerance to Effects of High-Dose Oral {Delta}9-Tetrahydrocannabinol and Plasma Cannabinoid Concentrations in Male Daily Cannabis Smokers. J Anal Toxicol. 2012.

[57] Montesinos P, Bergua JM, Vellenga E, Rayon C, Parody R, de la Serna J, et al. Differentiation syndrome in patients with acute promyelocytic leukemia treated with all-trans retinoic acid and anthracycline chemotherapy: characteristics, outcome, and prognostic factors. Blood 2009;113(4):775–83.